

1

Reply to the reviewer comments on the paper

2

”Long term dynamics of OH\* temperatures over Middle Europe: Trends and solar correlations”

3

4

by C.Kalicinsky et al.

5

We thank the referees for their helpful comments and recommendations. In the following, we discuss the issues addressed by the referees and explain our opinions and the modifications of our manuscript.

6

7

8

We enumerate the referee comments and repeat them in bold face. The modifications of the manuscript are displayed in the marked-up manuscript version as colored text. Deleted parts are shown in red and new text parts in blue.

9

10

11

## 1 Comments Referee 1

12

**This paper opens a new view on trends in mesopause temperatures. Since it is controversial in comparison with other results, possible open questions or weaknesses of the paper should be carefully revised. Therefore I recommend major revision but, on the other hand, I expect final publication of the paper even though my personal point of view in its area differs.**

13

14

15

16

17

1. **You assume that dependence of temperature on solar proxies is the same over the whole period of measurements. Some recent results indicate that it need not be true. Try to calculate solar proxy dependence separately for 1988-2005 and 2006-2015, even though the second period is rather short for significant result.**

18

19

20

21

22

23

24

25

26

27

28

29

30

31

32

33

34

35

36

37

38

39

We analysed if the assumption of a constant dependence of the temperature on solar proxies is true. The procedure we used is as follows. We take different time intervals with a length of 11 years, which is approximately the length of one solar cycle. We believe that this is the shortest time interval that can be used to derive significant results. The first time interval used is 1988 – 1998 and then we shift the interval several times by one year until the end of the whole time period is reached. For each time interval we derive the solar dependence and one linear trend. Here we follow the comments made by referee 2 that the non-orthogonal functions solar cycle and trend have to be fitted simultaneously. Thus, we use Eq. 3 for the fit. The results are presented in the manuscript in the new Fig. 14. The dependence on the solar proxy does not show significant changes during the whole time period of observations. The mean of the derived sensitivities is  $(3.9 \pm 0.3) \text{ K } (100 \text{ SFU})^{-1}$ , which agrees with the results obtained by fitting the solar dependence and one oscillation for the whole data set  $((4.1 \pm 0.8) \text{ K } (100 \text{ SFU})^{-1})$ . The derived trend values show an oscillation with the parameters  $A = (0.36 \pm 0.06) \text{ K}$  for the amplitude and  $P = (23.2 \pm 2.5) \text{ years}$  for the period. This oscillation agrees within the uncertainties with the period and phase of the derivative of the temperature oscillation derived by fitting the

1 solar dependence and one oscillation for the whole data set. Thus, the analysis  
2 by using 11-year time intervals confirms the results obtained by analysing the  
3 whole data set at once. In total, the assumption that the dependence of the  
4 temperature on solar proxies is the same over the whole period of observations  
5 appears to be correct for the Wuppertal OH\* temperatures.  
6 We added new Sects. 4.4 and 5.4 and presented the results of this analysis.

2. **It is natural that eq. (9) with three terms provides better fit than eq. (8) with two terms. Try to add to eq. (8) trend term as the third term and compare it with results of eq. (9).**

We added a trend term to Eq. 8:

$$T_0(SF, B_{solar}, t) = C_{solar} \cdot SF + C_{hale} \cdot B_{solar} + C_{trend} \cdot t + b,$$

7 The result by using this equation is not significantly different from the result by  
8 using the equation without the trend term. The  $r^2$  increases by only 0.001 and,  
9 thus, Eq. 9 explains still more variance of the temperature series. Furthermore,  
10 the obtained trend is not significantly different from zero. The obtained value is  
11  $C_{trend} = (-0.013 \pm 0.054) \text{ K year}^{-1}$ . Since the obtained trend is not significant,  
12 we keep at using the Eq. 8 as it is. We additionally added a sentence to Sect.  
13 4.3 to explain this fact.

- 14 3. **I do not agree with your conclusion (5) as it is written. The result**  
15 **that if you assume only one trend over the whole period than the**  
16 **trend depends on the length of period is trivial and well known but it**  
17 **does not mean that linear trend approach is wrong. Since long-term**  
18 **changes of some trend drivers (ozone, geomagnetic activity etc.) are**  
19 **temporally and spatially variable, trends can (and some must) change**  
20 **with time (see e.g. review paper Lastovicka et al. (2012)). For this**  
21 **reason a piecewise linear trend model with trend break(s) has been**  
22 **introduced, which you also apply. So either reformulate your conclu-**  
23 **sion (5) or delete it. Lastovicka, J., S.C. Solomon, L. Qian: Trends in**  
24 **the Neutral and Ionized Upper Atmosphere. Space Science Reviews,**  
25 **168, 113-145, doi: 10.1007/s11214-011-9799-3, 2012**

26  
27 We reformulated our conclusion 5) and we added a sentence to the introduction  
28 where we already describe the possibility of trend breaks and the use of piecewise  
29 linear trends.

- 30 4. **Page 7: The trend break near 1997 is not well supported by data in**  
31 **Fig. 8; it appears to be rather questionable.**

32  
33 The date 1997 is cited from Offermann et al., 2010. It is correct, that the possible  
34 trend break obtained by our analysis seems to occur earlier at about 1993/94.  
35 We reformulated the corresponding sentence.

1 **5. Figure 3: Have you some explanation for WUO-HPB difference in**  
2 **2008-2010?**

3 We believe that the difference is caused by some kind of local effects. The  
4 largest difference in 2010 for example is caused by an exceptional warm summer  
5 in Hohenpeissenberg. This larger temperatures in summer are also observed at  
6 the nearby station in Oberpfaffenhofen (see C.Schmidt et al., 2013, their Fig.  
7 12) but not in Wuppertal. We added a sentence about this fact to Sect. 2.3.

8 **6. Figures 8 and 9: Eye inspection of data points in these Figures calls**  
9 **for trend break rather in 2003 than in 2006, even though both are**  
10 **possible.**

11  
12 Due to the scatter of the data points, different break points seem to be possible.  
13 The new refined analysis, where all dependencies are fitted at once, leads to  
14 a break point in mid 2008, whereas the minimum of the 25-year oscillation is  
15 located at 2005/6. The break point given is the result of the best fit to the data  
16 series.

17 **7. You should also take into account results of some other authors:**

18 **C.M. Hall et al.: Temperature trends at 90 km over Svalbard, Nor-**  
19 **way (78 N, 16 E), seen in one decade of meteor radar observations.**  
20 **J. Geophys. Res., 117, D08104, doi: 10.1029/2011JD017028, 2012:**  
21 **No change of 90 km temperature trend over Svalbard around 2006.**  
22 **Meteor radar temperatures.**

23 **I.A. Mokhov, A.I. Semenov: Joint analysis of the long-term behavior**  
24 **of temperature in the mesopause and on the Earth's surface during the**  
25 **period of about 60 years. 6th NDMC Meeting, Grainau, 2014 (your**  
26 **co-author D. Offermann attended): 1960- 2012 data from Zvenigorod**  
27 **near Moscow. OH mesopause temperatures. Drop in the second half**  
28 **of the 1970s, than negative trend till the mid-1990s and essentially no**  
29 **trend afterwards. No change reported around 2006.**

30 **C.-Y. She, D.A. Krueger, T. Yuan: Long-term midlatitude mesopause**  
31 **region tem- perature trends deduced from quarter century (1990-**  
32 **2014) Na lidar observations. Ann. Geophysicae, 33, 363-369, doi:**  
33 **10.5194/angeocom-33-363-2015, 2015. Fort Collins/Logan, USA. 85-**  
34 **90 km temperature trend 1990-2014 is negative, after the mid- 1990s**  
35 **weaker than before. No change of trend reported around 2006.**

36  
37 We added comparisons with the mentioned publications (except for Mokhov et  
38 al., since it is not published) to the corresponding section dealing with linear  
39 trends and trend breaks (Sect. 5.2).

## 2 Comments Referee 2

The paper seeks to explore an alternative explanation for the change in slope of the OH temperature time series previously reported in earlier publications using a shorter time series. While the results are promising, I believe there is an overall shortcoming in the analysis technique. While this may not substantially change the overall results, it does put into question their statistical significance.

1. When fitting data using an orthogonal basis set, one can fit the functions simultaneously or sequentially, where the first function is subtracted from the data and the next fit to the residuals. However, in this paper there is a combination orthogonal functions (sinusoids in the case of the periodogram) and non-orthogonal functions (solar cycles and trends) fitted to the data sequentially. For example in Section 4.1, the solar 10.7 cm flux and a trend first are correctly fitted simultaneously as they are non-orthogonal. However, on page 7, lines 1-13, a periodogram, which fits a set of orthogonal sinusoids, is performed on the data that has had the solar and trend subtracted. It is not technically valid to perform the LSP of the residuals since functions non-orthogonal to the resulting periodogram sine waves have been removed. In particular, on line 5, it is stated that the LSP shows a peak with a period of 20 years remains after subtraction of the solar cycle and trend. However, the subtraction of a linear trend will act as a low pass filter (Kennedy, JGR 85, p219, 1980). Thus, the “peak” at 20 years is likely an artifact of passing the original data with its red-noise through this low pass filter.

Though the paper tries to justify this referring to Horne et al., 1986, it should be noted that Hornes’s analysis removed a function orthogonal to the other periodogram components. That is not the case here. Additionally, in Horne’s analysis, the estimate of variance after removal of the orthogonal function must be used to re-normalize the periodogram. That estimate of variance must be adjusted to the reduction in the number of degrees of freedom associated with the removal of these “correct” functions in much the same way that the total variance of the raw data set was estimated using N-1 to account for the removal of the mean. Here, a mean, a trend, and a solar cycle (itself a combination of several orthogonal sinusoids) have been removed, and the variance must be estimated appropriately.

We agree with the referee and made some corrections. Firstly, we calculated the variance of the raw data using N-1 degrees of freedom to account for the removal of the mean. This leads to a peak with a maximum of (N-1)/2 in case of a single sinusoid. So the FAP is described by

$$FAP = 1 - [1 - (\frac{2z}{N-1})^{(N-3)/2}]^{N_i},$$

1 since the samples taken from a gaussian distribution are processed in the same  
2 way as the original data series. Secondly, we adjusted the variance of the resid-  
3 uals by taking into account the number of parameters used in the fit subtracted  
4 from the data. We changed Sect. 3. and corresponding text parts.

5 Moreover, we removed all sequentially analysed parts and fitted all non-orthogonal  
6 functions simultaneously (see below at specific comments).

7 Lastly, we changed all parts where LSPs for residuals were analysed. We agree  
8 that the removal of functions non-orthogonal to the LSP sinusoids influence the  
9 LSP for the residuals. Therefore, remaining peaks are not interpreted as oscilla-  
10 tion with a specific period that remain or even are a component of the original  
11 data series. The LSPs for the residuals are only used to visualize the reduction  
12 in variance and to show the capability of different fits to reduce the large peak  
13 at 25-30 years in the periodogram for the original data series. A fit that takes  
14 into account all long term variations of the data series should remove all signals  
15 in the long periodic range of the LSP. The corresponding text parts in Sect. 4  
16 were changed to explain this.

- 17 **2. In section 4.2, the solar F10.7 cycle is not an orthogonal function to**  
18 **the two linear trends. Hence, its removal before fitting the two trends**  
19 **will influence the trends. All of these non-orthogonal components**  
20 **should be fit simultaneously.**

21  
22 We fitted the two linear trends and the dependence on the solar F10.7 cm flux  
23 simultaneously. The results slightly differ from the ones before. The new ana-  
24 lysis leads to the parameters  $C_{solar} = (3.3 \pm 0.9) \text{ K } (100 \text{ SFU})^{-1}$ ,  $C_{trend1} = (-$   
25  $0.24 \pm 0.07) \text{ K year}^{-1}$ , and  $C_{trend2} = (0.64 \pm 0.33) \text{ K year}^{-1}$ . The break point is  
26  $BP = (2008.8 \pm 1.7) \text{ years}$ . Thus, all of the results agree with the former results  
27 within the combined uncertainties. We changed the corresponding section 4.2.

- 28 **3. Similarly, in section 4.2, a sinusoid is fitted to the residual after re-**  
29 **moval on non-orthogonal components. It should be fit simultaneously**  
30 **with the other terms as in Equation 8.**

31  
32 The fit of the sinusoid is a hint to the best fitting period and amplitude of the  
33 oscillation. Thus, we kept this fit, but we fitted the oscillation together with the  
34 solar flux dependency and allowed the period to vary to derive the final result.  
35 See below point 6.

- 36 **4. Page 9, line 10, it is not mentioned whether this procedure explains**  
37 **more of the variance than the trend-break (assuming the trend break**  
38 **analysis is done correctly).**

39  
40 We now calculated the  $r^2$  of the trend break fit (0.74) and compared it to the  
41 other fits.

1 5. Page 9, line 13. As previous comments, one has not removed orthogo-  
2 nal functions nor adjusted the estimate of variance to account for the  
3 removal of these functions. Thus the LSP of the residual cannot be  
4 interpreted as periodic components remaining in the data. These may  
5 well have been created by the removal of the non-orthogonal functions.  
6

7 We changed the corresponding text part (see point 1).

8 6. Page 9, line 20. Again, the peak at 24 years in the periodogram could  
9 well be the result of the non-orthogonal functions being used to fit the  
10 data, and does not justify fixing the period to be fixed at 24 years in  
11 the fitting procedure. Thus, the period should also be allowed to vary  
12 in the fit in equation 9. Otherwise, there is no unambiguous evidence  
13 from the periodogram that it is exactly 24 years.  
14

We have done the fitting procedure again and allowed the period to vary.

$$T_0(SF, t) = C_{solar} \cdot SF + A \cdot \sin\left(\frac{2 \cdot \pi}{P}(t + \phi)\right) + b$$

15 The results of the new fit are  $C_{solar} = (4.1 \pm 0.8) \text{ K (100 SFU)}^{-1}$ ,  $A = (1.95 \pm 0.43) \text{ K}$ ,  
16 and  $P = (24.8 \pm 3.2) \text{ years}$ . Thus, all of the results are almost identical to the  
17 results obtained by fixing the period to 24 years. The  $r^2$  of the new fit is only  
18 slightly larger than before with a value of 0.775 (before 0.774).

19 7. In Section 4.4, , the LSP of the residuals is again not valid (as stated  
20 above), and these periods should not be fixed. One could fit a series  
21 of sinusoids simultaneously with the solar cycle, where the periods are  
22 also treated as free parameters. Using a non-linear least squares fit,  
23 the periodogram of the residuals may be used to estimate the initial  
24 values of these parameters. However, it is unclear whether there are  
25 enough degrees of freedom in the 25 data points to accommodate this  
26 analysis. I would advise that the fitting be performed simultaneously  
27 rather than sequentially to avoid the problems associated with the  
28 non-orthogonal basis set. In this way, the statistical significance of the  
29 periods, and the values of the periods themselves may be assessed. If  
30 indeed the results are substantially the same, then the interpretation  
31 will hold.

32 We fully agree with this comment and deleted Sect. 4.4 and also the discussion in  
33 Sect. 5.4, since a 25 data points series may not have enough degrees of freedom  
34 for a complete analysis of the MAOs together with the solar cycle and other  
35 components.

# Long term dynamics of OH\* temperatures over Middle Europe: Trends and solar correlations

Christoph Kalicinsky<sup>1</sup>, Peter Knieling<sup>1</sup>, Ralf Koppmann<sup>1</sup>, Dirk Offermann<sup>1</sup>, Wolfgang Steinbrecht<sup>2</sup>, and Johannes Wintel<sup>1</sup>

<sup>1</sup>Institute for Atmospheric and Environmental Research, University of Wuppertal, Germany

<sup>2</sup>DWD, Hohenpeissenberg Observatory, Germany

Correspondence to: C. Kalicinsky (kalicins@uni-wuppertal.de)

**Abstract.** We present the analysis of annual average OH\* temperatures in the mesopause region derived from measurements of the GRound based Infrared P-branch Spectrometer (GRIPS) at Wuppertal (51° N, 7° E) in the time interval 1988 to 2015. The current study uses a 7 year longer temperature time series compared to the latest analysis regarding the long term dynamics of OH\* temperatures measured at Wuppertal. This additional time of observation leads to a change in characterisation of the observed long term dynamics.

We perform a multiple linear regression using the solar radio flux F10.7cm (11-year cycle of solar activity) and time to describe the temperature evolution. The analysis leads to a linear trend of  $(-0.089 \pm 0.055) \text{ K year}^{-1}$  and a sensitivity to the solar activity of  $(4.2 \pm 0.9) \text{ K (100 SFU)}^{-1}$  ( $r^2$  of fit 0.6). However, one linear trend in combination with the 11-year solar cycle is not sufficient to explain all observed long term dynamics. Actually we find a clear trend break in the temperature time series in middle of 2006-2008. Before this break point there is an explicit negative linear trend of  $(-0.22 \pm 0.08) \text{ K year}^{-1}$  ( $-0.24 \pm 0.07) \text{ K year}^{-1}$  and after 2006-2008 the linear trend turns positive with a value of  $(0.38 \pm 0.23) \text{ K year}^{-1}$  ( $0.64 \pm 0.33) \text{ K year}^{-1}$ . This apparent trend break can also be described using a long periodic oscillation. One possibility is to use the 22-year solar cycle that describes the reversal of the solar magnetic field (Hale cycle). A multiple linear regression using the solar radio flux and the solar polar magnetic field as parameters leads to the regression coefficients  $C_{solar} = (5.0 \pm 0.7) \text{ K (100 SFU)}^{-1}$  and  $C_{hale} = (1.8 \pm 0.5) \text{ K (100 } \mu\text{T)}^{-1}$  ( $r^2 = 0.71$ ). But the best way to describe the OH\* temperature time series is to use the solar radio flux and a 24-year oscillation as an oscillation. A multiple linear regression using these parameters least square fit leads to a sensitivity to the solar activity of  $(4.3 \pm 0.7) \text{ K (100 SFU)}^{-1}$  ( $4.1 \pm 0.8) \text{ K (100 SFU)}^{-1}$  and an amplitude of the 24-year oscillation  $A = (1.95 \pm 0.43) \text{ K}$  ( $r^2 = 0.77$ ), a period  $P = (24.8 \pm 2.1) \text{ years}$ , and an amplitude  $C_{sin} = (1.95 \pm 0.44) \text{ K}$  of the oscillation ( $r^2 = 0.78$ ). The most important finding here is that using these parameters for the multiple linear regression this description an additional linear trend is no longer needed. Moreover, with the knowledge of this 24-25-year oscillation the linear trends derived in this and in a former study of the Wuppertal data series can be reproduced by just fitting a line to the corresponding part (time interval) of the oscillation. This actually means that depending on the analysed time interval completely different linear trends with respect to magnitude and sign can be observed. This fact is of essential importance for any comparison between different observations and model simulations.

After detrending the temperature time series regarding the 11-year solar cycle and the 24-year oscillation multi-annual oscillations

(MAOs) remain. A harmonic analysis finds three pronounced oscillations with periods of  $(2.69 \pm 0.06)$  years,  $(3.15 \pm 0.07)$  years, and  $(4.54 \pm 0.17)$  years. The corresponding amplitudes are  $(1.03 \pm 0.33)$  K,  $(1.03 \pm 0.33)$  K, and  $(0.91 \pm 0.36)$  K, respectively.

## 1 Introduction

The mesopause of the Earth is one of the most variable regions in the atmosphere. There are numerous different influences such as the solar radiation and different types of waves (e.g. tides, planetary waves, gravity waves) that affect the temperature in this region. Thus, the temperature undergoes large variations on very different timescales from minutes to years. The largest variation observed in temperature is the variation during one year. This seasonal variation is characterised by an annual, a semi-annual, and a ter-annual component (see e.g. Bittner et al., 2000) and shows maximum to minimum temperature differences of up to 60 K throughout a year (see Fig. 1). The second largest temperature variations are caused by different types of waves. The induced temperature fluctuations occur on timescales from days up to months in case of planetary waves (e.g. Bittner et al., 2000; Offermann et al., 2009; Perminov et al., 2014) and on the timescale of several minutes in case of gravity waves (e.g. Offermann et al., 2011; Perminov et al., 2014). Beside these rather short term fluctuations the temperature in the mesopause region also exhibits long term variations on the timescale of several years. Although the amplitudes of these long term variations are much smaller, the long term change of the mesopause temperatures is nevertheless clearly existent and important. Several previous studies showed the existence of an 11-year modulation of the temperature in coincidence with the 11-year cycle of solar activity which is visible in the number of sunspots and the solar radio flux F10.7cm (for a review of solar influence on mesopause temperature see Beig, 2011a). The reported sensitivities in the mid- to high-latitudes of the northern hemisphere lie between 1 to 6 K  $(100 \text{ SFU})^{-1}$ . Another type of long term change are linear trends in the analysed time interval. In the mesopause region of the northern hemisphere such trends range between about zero trend up to a cooling of 3 K  $\text{decade}^{-1}$  (for a review of mesopause temperature trends see Beig, 2011b). Also trend breaks seems to be possible, where the linear trend switches its sign (positive or negative trend) or the magnitude of the trend significantly changes (for an example of the latter case see Offermann et al., 2010). In case of such changes in trend (e.g. caused due to changes in trend drivers) a piecewise linear trend approach can be used, where different linear trends are determined for different time intervals (e.g. Lastovicka et al., 2012).

Beside these variations of the mesopause temperature Höppner and Bittner (2007) found a quasi 22-year modulation of the planetary wave activity which they derived from mesopause temperature measurements. This observed modulation coincides with the reversal of the solar polar magnetic field, the so-called Hale cycle. The solar polar magnetic field reverses every approximately 11 years at about solar maximum and, thus, the maximum positive and negative values of magnetic field strength occur in between two consecutive solar maxima (e.g. Svalgaard et al., 2005). Several studies showing a quasi 22-year modulation of different meteorological parameters such as temperature, rain fall, and temperature variability that are in phase with the Hale cycle or the double sunspot cycle (~~another type of Hale cycle with a period of about 22 years which is phase shifted compared to the Hale cycle of the solar polar magnetic field; the maxima and minima of the double sunspot cycle occur at maxima of the sunspot number (e.g. King, 1975; Qu et al., 2012)~~) exist (e.g. Willet, 1974; King et al., 1974; King, 1975; Qu

et al. , 2012), but no physical mechanism is found for these coincidences. The double sunspot cycle is another type of Hale cycle with a period of about 22 years which is phase shifted compared to the Hale cycle of the solar polar magnetic field. The maxima and minima of the double sunspot cycle occur at maxima of the sunspot number (e.g. King , 1975; Qu et al. , 2012). However, a number of possible influences also showing a 22-year modulation are named: galactic cosmic rays (GCR), solar irradiation, and solar wind (e.g. White et al., 1997; Zieger and Mursula , 1998; Scafetta and West , 2005; Miyahara et al. , 2008; Thomas et al. , 2013).

Because of this large number of influences and possible interactions the analysis of the temperatures is not easy to interpret, but due to the different timescales of the variations the different types of influences and phenomena can be distinguished sometimes. In this paper we focus on the long term variations of the mesopause temperature with timescales larger than  $\approx 10$  years. We use OH\* temperatures, which have been derived from groundbased measurements of infrared emissions at a station in Wuppertal (Germany) for our analyses.

The paper is structured as follows. In Sect. 2 we describe the instrument, the measurement technique, and show the OH\* temperature observations, Sect. 3 introduces the Lomb-Scargle periodogram and its properties, and in Sect. 4 we analyse the OH\* temperatures regarding solar correlations, long term trends, and long periodic as-well-as-multi-annual oscillations. A discussion of the obtained results is given in Sect. 5 and we summarise and conclude in Sect. 6.

## 2 Observations

### 2.1 Instrument and measurements

Excited hydroxyl (OH\*) molecules in the upper mesosphere/mesopause region emit radiation in the visible and near infrared. The emission layer is located at about 87 km height with a layer thickness of approximately 9 km (full width at half maximum) (e.g. Baker and Stair , 1998; Oberheide et al., 2006). The GRIPS-II (GRound based Infrared P-branch Spectrometer) instrument is a Czerny-Turner spectrometer with a Ge detector cooled by liquid nitrogen. It measures the emissions of the P1(2), P1(3), and P1(4) lines of the OH\*(3,1) band in the near infrared (1.524  $\mu\text{m}$ –1.543  $\mu\text{m}$ ) (for extensive instrument description see Bittner et al., 2000, 2002). The measurements are taken from Wuppertal (51° N, 7° E) every night with a time resolution of about 2 minutes. Thus, a continuous data series throughout a year is obtained with data gaps caused by cloudy conditions only. This results in approximately 220 nights of measurements per year (Oberheide et al., 2006; Offermann et al., 2010). The relative intensities of the three lines are used to derive rotational temperatures in the region of the OH\* emission layer (see Bittner et al., 2000, and references therein).

At the beginning of 2011 a newly build instrument was operated next to the GRIPS-II instrument. Simultaneous measurements conducted over a few months showed no significant differences between the two instruments. Unfortunately a detector failure stopped the GRIPS-II measurements mid of 2011, but the new instrument was able to continue the time series of nightly OH\* temperatures. Unfortunately, the new instrument had several technical problems in the following time which led to larger data gaps in the years 2012 and 2013. Finally, a reconstruction was performed to set up the GRIPS-N instrument, a Czerny-Turner spectrometer, equipped with a thermoelectrically cooled InGaAs detector. The optical and spectral properties of GRIPS-N and

GRIPS-II are very similar and, thus, the measurements of both instruments are nearly identical. The new GRIPS-N instrument was operated without further problems since begin of 2014. Hence, for the years 2014 and 2015 a complete set of measurements is available with only the typical data gaps due to cloudiness.

## 2.2 Data processing

- 5 The nightly average OH\* temperatures derived from the GRIPS-II and GRIPS-N measurements in Wuppertal are shown in the upper panel of Fig.1 for the time interval 1988 to 2015. As mentioned above the data series show larger gaps of several months due to technical problems in the years 2012 and 2013 and, additionally, a data gap of 3 months at the beginning of 1990. These years have to be excluded from the analysis, since a reasonable determination of an annual average temperature in presence of such large data gaps is not possible.
- 10 The by far largest variation in this temperature series is the variation in the course of a year. In order to evaluate the data with respect to long term dynamics with periods well above one year the seasonal variation has to be eliminated first. Since the temperature series exhibits data gaps mostly due to cloudy conditions, a simple arithmetic mean for each year is not advisable. We follow the method as used before in several analyses (e.g. Bittner et al., 2002; Offermann et al., 2004, 2006, 2010; Perminov et al. , 2014) and perform a harmonic analysis based on least square fits for each year separately. As described
- 15 in Bittner et al. (2000) the seasonal variation is characterised by an annual, a semi-annual and a ter-annual cycle. Thus, the temperature variation during one year is described by

$$T = T_0 + \sum_{i=1}^3 A_i \cdot \sin\left(\frac{2 \cdot \pi \cdot i}{365.25}(t + \phi_i)\right), \quad (1)$$

- where  $T_0$  is the annual average temperature,  $t$  is the time in days of year, and  $A_i, \phi_i$  are the amplitudes and phases of the sinusoids. By fitting this equation to the temperature data we can obtain the best possible estimate of the annual average
- 20 temperature  $T_0$  for each year. A year in this case denotes a calendar year. The resulting annual average temperatures are shown in the lower panel of Fig. 1 with data gaps in the years 1990, 2012 and 2013 (illustrated by the dashed lines). The seasonal variation of the year 2009 is shown in Fig. 2 as a typical example. As described above a detector failure in mid of 2011 stopped the GRIPS-II measurements. The following measurements were performed with a new instrument. The first year of full data coverage with GRIPS-N was 2014. Due to this the corresponding  $T_0$  for 2011 and 2014–2015 are marked in red in Fig. 1.

## 25 2.3 Comparison with other observations

- Since there is a data gap of two years (2012–2013) in the GRIPS-II and GRIPS-N measurements in Wuppertal and the last data points are derived from measurements by a new instrument, one has to ensure that the  $T_0$  from 2011 to 2015 fit the whole picture of the long term temperature evolution. We compare the Wuppertal observations with observations of OH\* temperatures taken from Hohenpeissenberg (48° N, 11° E) to check upon this. The instrument GRIPS-I in Hohenpeissenberg measures in the
- 30 same spectral range and uses the same data processing technique to determine OH\* temperatures. GRIPS-I is an Ebert-Fastie spectrometer with a liquid nitrogen cooled Ge detector (see e.g. Bittner et al., 2002). The measurements at Hohenpeissenberg

started end of 2003.

Figure 3 shows the comparison for the two measurement stations. A significant correlation between the two time series can be found with a correlation coefficient  $r = 0.72$ . The comparably low value of  $r$  is caused by the differences between 2007 to 2009, where the temperatures at Wuppertal partly decrease (increase) and the Hohenpeissenberg temperatures increase (decrease) at the same time. These differences are most likely caused by local effects. Furthermore, the largest absolute difference in 2010 is caused by an exceptional warm summer observed at Hohenpeissenberg. This warm summer is also observed at the nearby station in Oberpfaffenhofen (see Schmidt et al., 2013, their Fig. 12.) but not at Wuppertal.

The linear increase for each time series is shown in Fig. 3 as dashed line in black and red, respectively. In order to get the most appropriate comparison the linear fit to the Hohenpeissenberg time series only considers data points at times where measurements at Wuppertal are also available. The linear increase during the last 12 years at Wuppertal is  $(0.46 \pm 0.17) \text{ K year}^{-1}$  and the increase at Hohenpeissenberg is  $(0.42 \pm 0.16) \text{ K year}^{-1}$ . Both values agree very well, but the two lines are shifted towards each other indicating an offset between the two stations. This offset is about 0.9 K with Hohenpeissenberg being warmer. In a former study Offermann et al. (2010) obtained a mean offset between the two stations of 0.8 K for the time interval 2004–2008. Thus, this comparison agrees well the former study. Offermann et al. (2010) suggested the latitudinal difference between the stations to be responsible for this small difference. The temperature differences between the minima 2006 and the maxima 2014 also agree very well for both stations. The values are  $(7.3 \pm 0.7) \text{ K}$  at Wuppertal and  $(6.4 \pm 0.7) \text{ K}$  at Hohenpeissenberg. Since we analyse the relative evolution of the temperature series at Wuppertal the last data points fit the whole picture of the long term development of OH\* temperatures. Thus, the temperature increase observed at Wuppertal in the recent years is reliable and confirmed by the temperature increase observed at Hohenpeissenberg.

The latest analysis of the OH\* temperatures at Wuppertal regarding long term dynamics was performed for the time interval 1988–2008 (Offermann et al., 2010). The current study now considers a 7 year longer time series until 2015. The clear temperature increase during the last years has encouraged us to perform a new analysis regarding the long term dynamics.

### 3 Lomb-Scargle periodogram and false alarm probability

Analysing periodicities in the time series of  $T_0$  using the common Fast-Fourier-Transform (FFT) or wavelet analysis is not possible, since the time series exhibits data gaps and these methods rely on equidistant data. A frequently used method in such a situation is the Lomb-Scargle periodogram (LSP), which can handle time series with uneven spacing. The periodogram was developed by Lomb (1976) and Scargle (1982) and is equivalent to the fitting of sinusoids (Horne et al. , 1986). It can be calculated for every frequency  $f$ , which is another advantage compared to the discrete FFT, which is evaluated at discrete frequencies only. We use the algorithm by Townsend (2010) for the fast calculation of the periodogram.

An important quantity for the interpretation of a LSP is the so called false alarm probability (FAP). The FAP gives the probability that a peak of height  $z$  in the periodogram is caused just by chance, e.g. is caused by noise. As already pointed out by Scargle (1982), the cumulative distribution function (CDF) can be used to determine the FAP. If we take different samples of noise, calculate the LSP for each sample and then determine the height  $z$  of the maximum peak, the CDF of all these heights

$z$  gives the probability that there is a height  $Z$  smaller or equal to  $z$ . Consequently the value 1 - CDF gives the probability that there is a height  $Z$  larger than  $z$  by chance. Thus, 1 - CDF gives the FAP. Another important point in this context is the normalisation of the periodogram, since the normalisation affects the type of distribution of the periodogram and, thus, the description of the FAP (for a more detailed discussion see e.g. Horne et al. , 1986; Schwarzenberg-Czerny , 1998; Cumming et al. , 1999; Zechmeister and Kürster , 2009). We use the normalisation by the total variance of the data, which leads to a beta distribution in the case of gaussian noise (Schwarzenberg-Czerny , 1998). **Since a mean has to be subtracted from the data before calculating the LSP, the total variance is determined using N-1 degrees of freedom with N being the number of data points. This leads to a maximum value for a peak in the periodogram of (N-1)/2 in case of a single sinusoid. The FAP can be described by**

$$10 \quad FAP = 1 - \left[ 1 - \left( \frac{2z}{N-1} \right)^{(N-3)/2} \right]^{N_i}, \quad (2)$$

where  $N$  is the number of data points and  $N_i$  is the number of independent frequencies (Schwarzenberg-Czerny , 1998; Cumming et al. , 1999; Zechmeister and Kürster , 2009). The number of independent frequencies  $N_i$  has to be determined using simulations, since it is not possible to easily describe this quantity analytically (Cumming et al. , 1999). It depends on several factors, e.g. the number of data points  $N$  and the spacing of the data points. Horne et al. (1986) showed the partly large effect of the spacing (randomly or clumps of points) on  $N_i$ . Therefore, we perform simulations to determine  $N_i$  for the special situation of our observations. We take random values from a gaussian distribution **with mean zero and variance one** and the spacing of our observations as input. Then we calculate the LSP for ten thousand of such noise samples **in the same way as for the real data** and determine the height  $z$  of the maximum peak for each LSP. Every LSP is evaluated in the frequency range from Nyquist-frequency  $f = 1/2 \text{ year}^{-1}$  to  $f = 1/T \text{ year}^{-1}$ , where  $T$  in our case is 35 years, since we want to search for periodicities in range of the time window of the data series of 28 years. Periodicities in this range surely are accompanied with larger uncertainties, but the LSP gives a reasonable overview over the periodicities, even the large ones, included in the time series. The LSP is calculated at  $4T_{dur}\Delta f = 53$  evenly spaced frequencies in the mentioned frequency range, where  $T_{dur}$  is the duration of observations. Cumming et al. (1999) pointed out that this is an adequate sampling to observe all possible peaks. The upper panel of Fig. 4 shows the resulting empirical CDF of  $z$  for our sampling. The number of data points in this case is  $N = 25$  and the data series includes the data gaps in 1990 and 2012–2013. The lower panel of Fig. 4 displays the FAP (1 - CDF) as black curve. The fit of the theoretical curve using Eq. 2 to this data points is shown in red. The fit leads to a number of independent frequencies  $N_i = 32.4$ . With knowledge of  $N_i$  we can calculate the FAP for every peak height  $z$  and determine confidence levels for the LSP.

## 4 Analysis of long term dynamics: linear trend, solar correlations, long periodic and multi-annual oscillations

### 30 4.1 Linear trend and 11-year solar cycle

We analyse the long term trend and the correlation with the 11-year cycle in solar activity by means of a multiple linear regression. For this and the following analyses the time coordinate is shifted such as the first data point (1988.5) is set to zero.

The annual average temperatures are described by

$$T_0(t, SF) = C_{trend} \cdot t + C_{solar} \cdot SF + b, \quad (3)$$

where  $C_{trend}$  and  $C_{solar}$  are the two regression coefficients,  $t$  is the time in years,  $b$  is a constant offset, and  $SF$  is the solar radio flux F10.7cm in solar flux units (SFU). The solar radio flux is shown in Fig. 5 for the time interval from 1988 to 2015. There are three solar maxima in this time interval at about 1991, 2001 and 2014. This corresponds well to the annual average temperatures  $T_0$ , which also show local maxima at these points. The calculated regression coefficients determined by fitting Eq. 3 using the method of ordinary least squares are  $C_{trend} = (-0.089 \pm 0.055) \text{ K year}^{-1}$  and  $C_{solar} = (4.2 \pm 0.9) \text{ K (100 SFU)}^{-1}$ . The p-values (for the null hypothesis test) are 0.12 for  $C_{trend}$  and below 0.01 for  $C_{solar}$ . The whole fit has a  $r^2 = 0.6$ . Figure 6 shows the results for this analysis. The upper panel of the figure shows the temperature time series in black and the fit according to Eq. 3 in red. Additionally, the residual  $T_{res}$  is shown in the lower panel. Obviously, a fit taking into account a linear trend and the correlation with the 11-year solar cycle is a relatively poor fit to the temperature time series. The temperature residual still shows a temperature decrease until about 2005 and a temperature increase afterwards. Especially, the large increase at the end of the time series is not captured by the fit. Although there is an increase in solar activity in the same time interval, it is by far not enough to completely explain the observed temperature increase until 2015.

The obvious differences between fit and data series can also be seen in the LSPs in Fig. 7. The LSP is used here to analyse at which periods the determined fit reduces the variance of the original data series. The periodogram for the annual average temperatures  $T_0$  is shown in black and the periodogram for the residual  $T_{res}$  after subtracting the fit is shown in red. The LSP for the residual is normalised using the variance of the residual. All variances calculated for residuals in this study are adjusted to account for the reduction of degrees of freedom, which is caused by the subtraction of a fit, using the number of fit parameters. The peak at about 11 years in the LSP for  $T_0$ , which indicates the correlation with the 11-year solar cycle, disappeared after subtracting the fit. In contrast the large broad peak at the end of the periodogram is not completely removed. ~~and a peak at a period of about 20 years remains. Please note here, that the periodograms are normalised by the variance of the original time series and the residual, respectively. For the LSP for the residual this means, that the periodicities found and the corresponding false alarm probabilities are valid under the assumption that the fit used to build the residual is "correct" (see e.g. Horne et al., 1986).~~ Since the fit subtracted from the data may contain functions non-orthogonal to the LSP components, which are sinusoids, the remaining peak cannot be interpreted as an oscillation with a period of 20 years that remains or even is a component of the original data series. The peak is likely influenced by the fit subtracted from the data series, since e.g. the subtraction of a linear trend filters out low frequency components. But the clear signal in the long periodic range that remains in the periodogram shows that the fit determined by using Eq. 3 is not sufficient to remove all long term variations. There are two possibilities to describe the long term variation of the temperature series in a better way. Firstly, one can introduce a trend break so that there is a linear decrease in the first part and a linear increase in the second part of the series. Secondly, one can use a long periodic oscillation, which can introduce a trend break with a smoother transition. We will investigate these two possibilities in the next subsections.

## 4.2 Trend break

The trend break and the correlation with the 11-year solar cycle are analysed as follows. In a first step we determine the correlation with the 11-year solar cycle by a linear regression between the temperature time series and the solar radio flux. Thus, we remove the term  $C_{trend} \cdot t$  from Eq. 3. The regression coefficient is  $C_{solar} = (4.8 \pm 0.9) \text{ K} (100 \text{ SFU})^{-1}$  (p-value < 0.01).

In the second step we detrend the time series with respect to the 11-year solar cycle and fit two lines to the temperature residual to introduce the trend break. Since the year of the trend break, hereafter denoted as break point, is not known in advance, we use a variable break point and determine the best estimate by means of a least square fit. The residual after eliminating the 11-year cycle is shown in Fig. 8 in black. This residual is described by describing the annual average temperatures as

$$T_0(t, SF) = C_{solar} \cdot SF + \text{trend}_{2\text{phase}}(t), \quad (4)$$

where  $\text{trend}_{2\text{phase}}(t)$  is a trend term using two lines to introduce the trend break. The trend term is written as

$$\text{trend}_{2\text{phase}}(t) = \begin{cases} C_{trend1} \cdot t + b_1 & : t \leq BP \\ C_{trend2} \cdot t + b_2 & : t > BP \end{cases}, \quad (5)$$

where  $BP$  is the break point (in years). Since the two different lines need to be equal at the break point, this leads to the condition

$$\begin{aligned} C_{trend1} \cdot BP + b_1 &= C_{trend2} \cdot BP + b_2 \\ \Leftrightarrow b_2 &= b_1 + (C_{trend1} - C_{trend2}) \cdot BP \end{aligned} \quad (6)$$

Thus, Eq. 5 can be rewritten as

$$\text{trend}_{2\text{phase}}(t) = \begin{cases} C_{trend1} \cdot t + b_1 & : t \leq BP \\ C_{trend2} \cdot t + (b_1 + (C_{trend1} - C_{trend2}) \cdot BP) & : t > BP \end{cases}. \quad (7)$$

The description of the concept and the condition can be seen in Ryan and Porth (2007). Equation 4 now describes the temperature residual for annual average temperatures by using the correlation with the solar flux and a trend term with two different phases, where both phases have a linear temperature behaviour. These two phases are coupled by the variable break point  $BP$ .

We determine the best estimates for the parameters  $C_{solar}$ ,  $C_{trend1}$ ,  $C_{trend2}$ ,  $b_1$ , and  $BP$  by means of a least square fit. The fit leads to a sensitivity to the solar flux of  $C_{solar} = (3.3 \pm 0.9) \text{ K} (100 \text{ SFU})^{-1}$ . After subtracting this solar dependence and the mean the resulting residual and the best fit of the trend term are shown in Fig. 8 as black and red line, respectively. Additionally, the position of the break point and the corresponding uncertainties are marked as vertical black line and vertical dashed black lines, respectively. We observe a trend break in the middle of year 2006 ( $BP = (2006.7 \pm 2.4) \text{ year}$ ). 2008

( $BP = (2008.8 \pm 1.7)$  year). Before the trend break in ~~2006~~ 2008 there is a negative temperature trend  $C_{trend1} = (-0.22 \pm 0.08) \text{ K year}^{-1}$   $(-0.24 \pm 0.07) \text{ K year}^{-1}$  and after the break point the trend is positive with a slope  $C_{trend2} = (0.38 \pm 0.23) \text{ K year}^{-1}$   $C_{trend2} = (0.64 \pm 0.33) \text{ K year}^{-1}$ . The  $r^2$  of the whole fit is 0.74. The LSP for the residual after subtracting the trend break fit is shown in Fig. 9 in red. The former large peak at the right end of the periodogram for the original data series (black curve) is nearly completely removed after subtracting the trend break fit. Thus, the fit using two linear trends and a trend break explains a large portion of the long term variation of the OH\* temperature series. ~~These findings are also in good agreement with the observations at Hohenpeissenberg, where the temperature series (not corrected for 11-year solar cycle) also shows a minimum at date 2006.5 and an increase afterwards (compare Fig. 3).~~

### 4.3 Long term oscillation

10 We analyse the possibility of an oscillation instead of a trend break. ~~Thus,~~ In order to get an idea about the oscillation we fit a sinusoid of the form

$$T_{res}(t) = A \cdot \sin\left(\frac{2 \cdot \pi}{P}(t + \phi)\right) + b \quad (8)$$

to the temperature residual after subtracting the solar dependence and the mean (see Fig. 8 black curve).  $A$  denotes the amplitude,  $P$  the period, and  $\phi$  the phase. Additionally, we fit an offset  $b$ , since the mean of the temperature residual is not necessarily identical with the zero crossing of the oscillation. The resulting oscillation is shown in Fig. 8 as blue curve. The important estimated parameters of the fit are an amplitude  $A = (1.89 \pm 0.43) \text{ K}$   $(2.06 \pm 0.43) \text{ K}$  and a period of about ~~24~~ 26 years ( $P = (23.6 \pm 2.6) \text{ years}$ )  $(26.3 \pm 3.2) \text{ years}$ ). Obviously, this oscillation and the fit using the two linear phases and a trend break (red lines in Fig. 8) are nearly identical for the time interval after ~~2006~~ 2008. Before ~~2006~~ 2008 the blue curve oscillates about the red line. Additionally, the oscillation introduces a much smoother transition from decreasing to increasing temperatures. The decrease in variance is larger for the oscillation than for the fit using two linear phases. The variances of the two resulting differences,  $T_{res}$  minus linear trends (red lines) and oscillation (blue curve), respectively, are ~~2.4 K<sup>2</sup>~~  $2.11 \text{ K}^2$  and ~~1.9 K<sup>2</sup>~~  $1.96 \text{ K}^2$ . Thus, the oscillation describes  $T_{res}$  better, especially at the beginning of the time series. Offermann et al. (2010) already suggested a trend break in the temperature series at about 1997. ~~and~~ The oscillation would account for such a second trend break in the temperature series in the mid nineties at about 1993.

25 Very prominent is the fact, that the oscillation has a period of about ~~24~~ 26 years with a minimum at about ~~2005~~ 2006 and a maximum at about 1993/~~1994~~. This type of oscillation with very similar parameters can be found on the sun. The original solar cycle (Hale cycle) is a cycle with a period of about 22 years and describes the reversal of the magnetic field of the sun. The solar polar magnetic field of the sun is shown in Fig. 8 as green curve with a second axis to the right. Evidently, the oscillation fitted to  $T_{res}$  and the Hale cycle of the magnetic field are very similar in the time interval shown. The correlation coefficient for a linear regression between the magnetic field and the temperature residual (black curve in Fig. 8) is  $r = -0.6$  0.55. The corresponding slope is ~~(1.8 ± 0.5) K (100 μT)<sup>-1</sup>~~  $(1.74 \pm 0.56) \text{ K (100 } \mu\text{T)}^{-1}$  (p-value < 0.01). This is a remarkable accordance between the observed oscillation in atmospheric temperature and solar polar magnetic field.

The long periodic oscillation describes the largest part of the temperature variability after detrending the temperature series

with respect to the 11-year solar cycle. Thus, we analyse the temperature series  $T_0$  by means of a multiple linear regression again to fit all dependencies simultaneously. and We include the solar polar magnetic field in the equation, which replaces the linear trend. Hence, Eq. 3 transforms to

$$T_0(SF, B_{solar}) = C_{solar} \cdot SF + C_{hale} \cdot B_{solar} + b, \quad (9)$$

5 where  $B_{solar}$  denotes the solar polar magnetic field and  $C_{hale}$  the corresponding regression coefficient. The analysis leads to the results for the regression coefficients  $C_{solar} = (5.0 \pm 0.7) \text{ K } (100 \text{ SFU})^{-1}$  and  $C_{hale} = (1.8 \pm 0.5) \text{ K } (100 \mu\text{T})^{-1}$ . ~~Both regression coefficients are significant with corresponding p-values below 0.01 and they agree within the uncertainties with the coefficients, which are determined one after the other as shown above.~~ The fit to the temperature time series has a  $r^2 = 0.71$ . This value is larger than the value for the fit including the 11-year solar cycle and one linear trend, which has a  $r^2 = 0.6$  (see  
10 Sect. 4.1) ~~Hence, the new description with the solar polar magnetic field as parameter explains more variance of the temperature series.~~, but it is slightly lower than the  $r^2 = 0.74$  of the trend break fit (see Sect. 4.2). An additional linear trend added to Eq. 9 does not significantly change the results. The obtained linear trend is insignificant in this case and, therefore, it is excluded. The resulting fit and the residual are shown in Fig. 10. The fit curve (red colour) shows good agreement with the long term variation of the temperature (black dots), but there are still some obvious differences, especially at the beginning of the time series.  
15 Additionally, the temperature residual (lower panel of Fig. 10) seems to show a long periodic oscillation. ~~This is confirmed by the LSP for the residual, which is shown in Fig. 11. A small peak at the right end of the periodogram remains. There are two possibilities that explain this remaining peak. Firstly, there is a second oscillation besides the Hale cycle. Secondly, and this is the most likely explanation, there is only one oscillation with a period similar to the Hale cycle but phase shifted. This explanation is supported by the fact, that the oscillation fitted to the temperature residual after subtracting the 11-year solar cycle (blue curve in Fig. 8) is slightly phase shifted to the Hale cycle (green curve in Fig. 8). Both the maximum and the minimum of the fitted sinusoid occur somewhat before the extrema in the solar polar magnetic field. The LSP for the residual (red curve in Fig. 11) shows that the former large peak at the long periodic end of the periodogram (black curve) is largely reduced after subtracting the fit, which shows that the description using the 11-year solar cycle and the Hale cycle explains most of the variance in the long periodic range. But, possibly, an oscillation with similar parameters than the Hale cycle which  
20 are slightly changed (in amplitude, phase and/or period) can describe the annual average temperatures even better.~~

We analyse ~~the second~~ this possibility and add an oscillation ~~with a fixed period of 24 years (equal to the period of the fit to the temperature residual) to the multiple linear regression,~~ to the temperature description, which replaces the solar polar magnetic field. Since the oscillation and the 11-year solar cycle are non-orthogonal functions we fit here all dependencies simultaneously.

The equation transforms to

$$30 \quad T_0(SF, t) = C_{solar} \cdot SF + C_{sin} \cdot \sin\left(\frac{2 \cdot \pi}{P}(t + \phi)\right) + b, \quad (10)$$

where  ~~$C_{sin}$  and  $C_{cos}$  are the amplitudes~~ is the amplitude,  $P$  is the period, and  $\phi$  is the phase of the oscillation, and  $t$  is the time in years. ~~The sum of the sine wave and the cosine wave with fixed period and phases but free amplitudes is one sinusoid with period of 24 years and a free phase ( $A \cdot \sin(\frac{2 \cdot \pi}{24} \cdot t + \phi)$ ).~~The resulting regression coefficients The results of the least

square fit are  $C_{solar} = (4.3 \pm 0.7) \text{ K} (100 \text{ SFU})^{-1}$   $(4.1 \pm 0.8) \text{ K} (100 \text{ SFU})^{-1}$  (p-value  $\ll 0.01$ ) for the sensitivity to the solar activity, and  $C_{sin} = (1.92 \pm 0.43) \text{ K}$   $(1.95 \pm 0.44) \text{ K}$ , and  $C_{cos} = (0.34 \pm 0.42) \text{ K}$  for the amplitude of the sine and cosine wave, and  $P = (24.8 \pm 2.1) \text{ years}$  for the period of the oscillation. Thus, the amplitude of the 24-year oscillation is  $A = (1.95 \pm 0.43) \text{ K}$  ( $A = \sqrt{C_{sin}^2 + C_{cos}^2}$ ). The obtained oscillation will be hereafter denoted as 25-year oscillation. The fit has a  $r^2 = 0.77$   $0.78$ , which is a substantial increase and the largest value of  $r^2$  obtained. The fit and the residual are shown in Fig. 12. The temperature residual (lower panel of Fig. 12) shows no obvious long term variation any more, neither a linear trend nor an oscillation. Only some variations with periods on the order of several years remain. The LSP for the temperature residual, which is shown in Fig. 13, confirms this. All long term variations with periods larger than about 10 years are now removed from the temperature series. There are only peaks in the range up to a period of about 8 years. Thus, the description of the annual average temperature including the 11-year solar cycle and an oscillation with a period of 24-25 years is sufficient to explain all long term variations. No further linear trend can be found in the data series.

#### 4.4 Multi-annual oscillations

We briefly analyse the oscillations that remain after subtracting the long term variations. These oscillations have periods in the range of several years and we therefore denote them as multi-annual oscillations (MAO). The LSP for the temperature residual (see red curve in Fig. 13) shows three distinct peaks. The first peak is located at a period of about 2.7 years, the second peak is located at about 3.1 years, and the last pronounced peak belongs to a period of about 4.5 years. The FAPs for all peaks is very high with values of slightly below 50% or even higher. But the determination of the FAP (see Sect. 3) is based only on the maximum peak found in a periodogram calculated for noise and there is no additional consideration of other peaks found in the periodogram, which may have a similar height as the maximum peak. If you have a superposition of several sinusoids each with same or similar amplitude, the FAP for one of the corresponding peaks will increase with increasing number of sinusoids. As an example, the height of the peak in a LSP for a single sinusoid is  $N/2$ , with  $N$  as number of data points (see e.g. Horne et al., 1986). If you add other sinusoids with same amplitude but different period, the heights of the peaks in the LSP will decrease. Taken 25 data points, as it is the case for the GRIPS measurements, the height of the peak for a single sinusoid is 12.5, for two sinusoids (periods e.g.: 3.0 and 5.0 years) the peak heights of both peaks are approximately 6.5, and for three sinusoids (periods e.g.: 3.0, 5.0, and 7.0 years) the peak heights are only about 4.5. The peak height additionally depends on the phases of the different sinusoids, and therefore on the different superposition. Thus, the numbers given are approximations. Nevertheless, the general decrease in height with increasing number of sinusoids is obvious. As a result the FAP for such peaks detected for a superposition of sinusoids would be high, although all oscillations are real. In the case of the temperature residual and the resulting LSP (see red curve in Fig. 10) you get a similar picture. There are several peaks with similar height, which could be caused by a superposition of sinusoids with similar amplitudes, although the FAP for a single peak is high. We use harmonic fits to get estimates for the three identified MAOs in the temperature residual after removing the 11-year cycle and the 24-year oscillation. A harmonic fit to the temperature residual initiated at a period of 2.7 years leads to the results  $P = (2.69 \pm 0.06) \text{ years}$  and  $A = (1.03 \pm 0.33) \text{ K}$ , a harmonic fit initiated at a period of 3.1 years results in the parameters  $P = (3.15 \pm 0.07) \text{ years}$  and  $A = (1.03 \pm 0.33) \text{ K}$ , and a harmonic fit initiated at a period of 4.5 years results in the parameters

$P = (4.54 \pm 0.17)$  years and  $A = (0.91 \pm 0.36)$  K. Thus, the amplitudes of all three oscillations are very similar. This would explain the observed LSP, where we can see clear peaks, but the FAP of each peak is very high. As explained above this behaviour is expected for a superposition of several sinusoids. Furthermore, if one subtracts one of the fitted oscillations from the temperature residual and calculates the LSP for the resulting difference, the peak corresponding to the subtracted oscillation is removed, whereas the two other peaks remain. Since this holds for all combinations, we believe that all three MAOs found in the data are real and no artefacts or leakage effects. These three MAOs are the main part of the temperature variance after eliminating the long term variations. But in comparison to the long term variations the observed amplitudes of the MAOs are much smaller, by about a factor of two. Hence, the whole observed temperature variation is dominated by the long term variations and the MAOs have only minor contribution.

#### 4.4 Stability of solar sensitivity

In the former sections a constant sensitivity to the solar activity for the complete observations was assumed. In order to study if this assumption is correct and the oscillation derived in Sect. 4.3 is also found allowing a varying solar sensitivity, we analyse the time series of annual temperatures again. For the analysis we use time intervals of 11 years (approximately the length of one solar cycle). We start with the interval 1988 – 1998 and always shift the time interval by one year ending with the interval 2005 – 2015. Time intervals that do not cover a 11-year window because of missing data at the end or beginning of the interval are excluded from the analysis. All possible time intervals are analysed separately. The temperatures in each interval are described by Eq. 3 and the coefficients  $C_{trend}$  and  $C_{solar}$  are determined. By doing this, we assume a linear trend in each time interval, but the trend and the sensitivity to the solar activity are allowed to vary from one interval to the next.

The results of the analysis are shown in Fig. 14. The sensitivity to the solar activity is shown in the upper panel of the figure in black and the grey shaded area marks the range for the sensitivity derived in Sect. 4.3 for the best fit  $((4.1 \pm 0.8) \text{ K } (100 \text{ SFU})^{-1})$ . The sensitivities derived for the 11-year time intervals show some variations but considering the uncertainties no significant changes can be observed. The mean of the derived sensitivities is  $(3.9 \pm 0.3) \text{ K } (100 \text{ SFU})^{-1}$  which agrees very well with the value derived before.

The lower panel of Fig. 14 shows the derived linear trends in black. We fit a sinusoid to these trend values (red line in figure) that results in the values  $A = (0.36 \pm 0.06) \text{ K}$  for the amplitude and  $P = (23.2 \pm 2.5) \text{ years}$  for the period. This oscillation found in the trend values should be equal to the derivative of the 25-year oscillation derived in Sect. 4.3 with a reduced amplitude, since 11-year time intervals are used and so no local derivative is obtained. This agreement is indeed the case. The observed period of the trend oscillation agrees within the uncertainties with the 25-year oscillation derived in the former section and also the phase is correct. The 25-year oscillation of the temperature is shown in the lower panel of Fig. 14 in blue and the corresponding derivative in green (with a second axis to the right). Obviously the green and the red curve are nearly identical. In total the analysis method using 11-year time intervals leads to the same results as the fit including the sensitivity to the solar cycle and an oscillation to the whole data series. So this analysis confirms the results obtained in Sect. 4.3.

## 5 Discussion

### 5.1 11-year solar cycle

There are numerous publications about the correlation of the 11-year cycle of solar activity and temperatures in the mesopause region. A review is given by Beig (2011a, see Fig. 2 and corresponding section). The sensitivity to the solar activity in the northern mid- to high-latitudes reported in this review is about 1–6 K (100 SFU)<sup>-1</sup>. In a more recent study on mesopause temperatures measured at Zvenigorod (56° N, 37° E; 2000–2012) by Perminov et al. (2014) a sensitivity of  $(3.5 \pm 0.8)$  K (100 SFU)<sup>-1</sup> is found. This value perfectly agrees with the result of a former analysis of the GRIPS measurements at Wuppertal (1988–2008), where also a sensitivity of  $(3.5 \pm 0.2)$  K (100 SFU)<sup>-1</sup> was found (Offermann et al., 2010). In our study we obtained results in the range between 4–5 K (100 SFU)<sup>-1</sup>. Depending on the analysis method the results slightly differ from each other, but they nearly all agree within the uncertainties (only the value derived by using the Hale cycle seems to be a little to large). Since the parameters for the multiple-linear-regressions fits (solar radio flux, solar polar magnetic field, 24-year oscillation, and time) are not completely independent of each other, the derived regression coefficients are good only approximations to the “true” values. Much longer time series including more solar maxima would be necessary to finally derive the “true” regression coefficients. Thus, small differences in the derived values are expected, especially in the case of the multiple linear regression including the solar radio flux and the linear trend, since this regression leads to a result that cannot completely explain all long term trends and oscillations in the time series. Nearly all derived values for the sensitivity of the OH\* temperatures to the 11-year solar cycle are slightly larger than the one derived in the former analysis of the GRIPS measurements at Wuppertal. But the time intervals are different for the analyses, which can lead to different results for the derived sensitivities. This aspect was already discussed by Offermann et al. (2010).

Although Beside the fact that the derived values are in the expected range for northern mid- to high-latitudes, one new aspect with respect to the correlation between 11-year solar cycle and mesopause temperatures has become apparent. In the present study the correlation was determined for three solar maxima including the comparably weak latest solar cycle 24. Our study shows that the significant correlation between OH\* temperatures and the 11-year solar cycle is still evident in this case.

### 5.2 Linear trend and trend break

Temperature trends in the mesopause region are reported in a number of papers, and a review about numerous results is given by Beig (2011b, see Fig. 2 and corresponding section). The temperature trends reported there range between no trend up to a cooling of about 3 K decade<sup>-1</sup>. The recent analysis Recent studies by different authors lead to the following results. Combined Na lidar observations at Fort Collins (41° N, 105° W) and Logan (42° N, 112° W) in the time interval 1990–2014 lead to an insignificant trend of  $(-0.64 \pm 0.99)$  K decade<sup>-1</sup> at 85 km and the negative trend increases with increasing height up to a maximum of  $(-2.8 \pm 0.58)$  K decade<sup>-1</sup> at 91 and 93 km (She et al., 2015). The analysis by Perminov et al. (2014) for the measurements at Zvenigorod (56° N, 37° E) showed a trend of  $(-2.2 \pm 0.9)$  K decade<sup>-1</sup> for the time interval 2000–2012. Hall et al. (2012) derived a trend of  $(-4 \pm 2)$  K decade<sup>-1</sup> from meteor radar observations over Svalbard (78° N, 16° E) at 90 km for the time intervall 2001–2012. In a former study of the Wuppertal OH\* temperature series (1988–2008) a negative trend of

( $-2.3 \pm 0.6$ ) K decade<sup>-1</sup> was found (Offermann et al., 2010). The multiple linear regression using the solar radio flux and time as parameters in this paper results in a cooling trend of ( $-0.89 \pm 0.55$ ) K decade<sup>-1</sup> for the Wuppertal OH\* temperatures from 1988 to 2015 (see Sect. 4.1), which is in good agreement with the observations by She et al. (2015). The value is significantly smaller than the trend derived in the former study of the Wuppertal data. Since there is an increase in temperature since about 2006 and the former study by Offermann et al. (2010) ended 2008, this temperature increase leads to a smaller negative trend in our study. But as shown above one linear trend is not sufficient to account for all long term variation in the time series. Due to this we introduced a trend break and found a negative trend before year 2006 2008 and a positive trend afterwards. The obtained values are ( $-2.2 \pm 0.8$ ) K decade<sup>-1</sup> ( $-2.4 \pm 0.7$ ) K decade<sup>-1</sup> and ( $3.8 \pm 2.3$ ) K decade<sup>-1</sup> ( $6.4 \pm 3.3$ ) K decade<sup>-1</sup>, respectively (see Sect. 4.2). The time interval used in the former study of the Wuppertal OH\* temperature series by Offermann et al. (2010) is nearly identical with the time interval of the first phase showing the negative temperature trend. The linear temperature trends derived by Offermann et al. (2010) and in this study for this time interval perfectly agree. Due to the additional 7 years of observations this study now clearly shows that the former negative linear trend turned into a positive trend in the last years. This finding is contrary to the other recent studies (She et al., 2015; Perminov et al., 2014; Hall et al., 2012), where no trend break in mid 2000's is reported.

### 5.3 Long term oscillation

The observed trend break can also be described using a long periodic oscillation. In Sect. 4.3 we show two different possibilities for such a long periodic oscillation.

Firstly, the solar polar magnetic field (Hale cycle) is used as one parameter in a multiple linear regression with the second parameter being the solar radio flux. The correlation coefficients are  $C_{solar} = (5.0 \pm 0.7)$  K (100 SFU)<sup>-1</sup> and  $C_{hale} = (1.8 \pm 0.5)$  K (100 μT)<sup>-1</sup> ( $r^2 = 0.71$ ). But especially at the beginning of the time series the fit curve is not perfectly matching the observations (see Fig. 10). Additionally, the LSP for the temperature residual after subtracting this fit curve still shows a peak corresponding to a long period in the long periodic range. (red curve in Fig. 11). Thus, the Hale cycle together with the 11-year solar cycle cannot explain all observed long term dynamics. Because of these facts, we believe that the solar polar magnetic field as acting input parameter is not very likely.

Secondly, an independent oscillation with a period of 24 years is used to describe the OH\* temperature time series. A multiple linear regression least square fit using the solar radio flux and this 24-year an oscillation with free amplitude, period, and phase leads to the regression coefficients  $C_{solar} = (4.3 \pm 0.7)$  K (100 SFU)<sup>-1</sup> ( $4.1 \pm 0.8$ ) K (100 SFU)<sup>-1</sup> and an amplitude of the oscillation  $A = (1.95 \pm 0.43)$  K,  $C_{sin} = (1.95 \pm 0.44)$  K for the amplitude, and  $P = (24.8 \pm 2.1)$  years for the period. ( $r^2 = 0.77$  0.78). After subtracting the derived fit curve the LSP for the residual does not show any remaining long periodic signals (see Fig. 13). The 24 obtained 25-year oscillation, shown in Fig. 15 as black curve (with full circles), is phase shifted compared to the Hale cycle and the extrema occur slightly before the extrema of the solar polar magnetic field (compare Fig. 8 green curve and Fig. 15 black curve; e.g. maximum at about 1993 compared to 1994/1995). This time shift supports the opinion that the Hale cycle is not very likely as an acting input parameter. The nature of the 24 25-year oscillation is not clear yet, but a selfsustained oscillation in the atmosphere would be a real possibility. Such oscillations were recently discovered by

Offermann et al. (2015). An oscillation with a period of about 20 to 25 years is found in various atmospheric parameters such as temperature (Qu et al. , 2012; Wei et al. , 2015), geopotential height (Coughlin and Tung , 2004a, b), and planetary wave activity (Jarvis , 2006; Höppner and Bittner , 2007). It is also seen in two atmospheric models (HAMMONIA, WACCM). A detailed discussion is, however, beyond the scope of this paper.

5 The most important point here is that no additional linear trend can be maintained. All long term dynamics of the Wuppertal OH\* temperature time series can be described as a combination of the 11-year solar cycle and a 24 25-year oscillation. With the knowledge of this 24 25-year oscillation the linear trends derived in this study (see Sect. 4.1) and a former study of the Wuppertal OH\* temperature time series can be reproduced. Figure 15 demonstrates that very different trends can be ~~calculated~~ obtained if specific time intervals of the (sinusoidal) data are used. By fitting a line to the corresponding part (time interval) of the data we  
10 obtain the linear trend. The linear trend for the time interval analysed in this study (1988–2015) is  $(-0.087 \pm 0.033) \text{ K year}^{-1}$   $(-0.097 \pm 0.032) \text{ K year}^{-1}$ , which is ~~identical to the same as~~ the linear trend  $C_{trend} = (-0.089 \pm 0.055) \text{ K year}^{-1}$  derived by using a multiple linear regression with time and solar radio flux as parameters (see Sect. 4.1). This linear trend is shown in Fig. 15 as red line (with squares). Offermann et al. (2010) derived a linear trend for the time interval 1988–2008 of  $(-0.23 \pm 0.06) \text{ K year}^{-1}$ . A linear fit to the data for this time interval leads to a slope of  $(-0.21 \pm 0.03) \text{ K year}^{-1}$   $(-0.22 \pm 0.03) \text{ K year}^{-1}$  (green line (with triangles) in Fig. 15). Thus, the 24 25-year oscillation “explains” the derived linear trends of this and the former study as well as the obvious trend break observed in ~~2006 the data series~~. This means that all different kinds of linear trends are possible depending on the time interval which is analysed. If we continue the oscillation back to 1975 (black dashed line in Fig. 15) and fit a line to these “data” for the whole time interval (1975–2015; blue line (with plus signs)) in Fig. 15), this leads to a slope of  $(0.015 \pm 0.012) \text{ K year}^{-1}$   $(0.017 \pm 0.018) \text{ K year}^{-1}$ . Surely, this continuation  
15 is an assumption and cannot be verified by the observations, but it is likely and clearly shows the possible effects. The presence of such a long periodic oscillation that in combination with the 11-year solar cycle explains all long term dynamics without an additional linear trend is very important with respect to any kind of comparison between different observations or model simulations. Each comparison of linear trends is only valid if the same time interval is analysed. Furthermore, the current study suggests that there is no universal linear trend which is valid for all time intervals at this altitude.  
20

#### 25 5.4 Multi-annual oscillations

~~After detrending the OH\* temperature series regarding the long term variations (11-year solar cycle and 24-year oscillation) MAOs with periods below 8 years remain. The most prominent oscillations have periods of  $P = (2.69 \pm 0.06)$  years,  $P = (3.15 \pm 0.07)$ , and  $P = (4.54 \pm 0.17)$  years with corresponding amplitudes of  $A = (1.03 \pm 0.33) \text{ K}$ ,  $A = (1.03 \pm 0.33) \text{ K}$ , and  $A = (0.91 \pm 0.36) \text{ K}$ , respectively. In a recent study we analysed the SABER temperatures in the region  $45^\circ \text{ N} - 55^\circ \text{ N}$  and  $4^\circ \text{ W} - 16^\circ \text{ E}$  in the time  
30 interval from 2002 to 2012 (see Offermann et al., 2015). Beside oscillations with other periods the SABER temperatures show a MAO with a period of about 2.6 years and an amplitude of about 1 K in altitude range between 80 to 90 km. Thus, there is an good agreement between this MAO and the MAO with period of about 2.69 years found in the GRIPS observations. The study by Offermann et al. (2015) indicates that the MAOs identified in the atmosphere are selfsustained oscillations, since they are also present in model simulations by the HAMMONIA model with climatological boundary conditions.~~

## 5.4 Stability of solar sensitivity

The analysis by using different 11-year time intervals leads to two main results. Firstly, the sensitivity to the solar activity is fairly stable throughout the whole time period 1988 – 2015. There are some variations in the sensitivity but considering the uncertainties there are no significant changes. The mean of the derived values is  $(3.9 \pm 0.3) \text{ K (100 SFU)}^{-1}$ . This value is in nearly perfect agreement with the result of  $(4.1 \pm 0.8) \text{ K (100 SFU)}^{-1}$  for the best fit (11-year solar cycle and the 25-year oscillation) using the whole data series at once. So the assumption that the sensitivity to the solar activity is constant during the whole time period is valid for the Wuppertal OH\* observations.

Secondly, the derived partial trend values show the same oscillation as the derivative of the 25-year temperature oscillation. Thus, the analysis using the 11-year time intervals confirms the result that beside the 11-year solar cycle an oscillation of about 25 years is the second important component of the OH\* temperatures observed at Wuppertal.

## 6 Summary and conclusions

We present the analysis of the OH\* temperatures derived from the GRIPS measurements at Wuppertal. We use annual average temperatures in the time interval 1988 to 2015 for our study. The study mainly focuses on the long term dynamics as well as on MAOs with periods between 2 to 5 years. The analysis and leads to the following results:

1. The OH\* temperatures show a significant correlation with the solar radio flux. We find a sensitivity to the 11-year solar cycle of  $4.3 \pm 0.5 \text{ K (100 SFU)}^{-1}$ .
2. One linear trend during the whole time interval (together with the sensitivity to the 11-year solar cycle) cannot sufficiently explain all long term dynamics found in the OH\* temperatures. We introduce a trend break to better account for these long term dynamics. The best representation of the temperature series is found if the trend break occurs in mid 2006 (date =  $(2006.7 \pm 2.4) \text{ years}$ ) 2008 ( $BP = (2008.8 \pm 1.7) \text{ years}$ ). Before the break point the linear trend is negative and after the break point the trend turns positive with the slopes of  $(-0.22 \pm 0.08) \text{ K year}^{-1}$  ( $-0.24 \pm 0.07) \text{ K year}^{-1}$  and  $(0.38 \pm 0.23) \text{ K year}^{-1}$  ( $0.64 \pm 0.33) \text{ K year}^{-1}$ , respectively.
3. The reversal of the temperature trend can also be described as by a long periodic oscillation. We present two possibilities for this oscillation. Firstly, the solar polar magnetic field of the sun (Hale cycle) is used in a multiple linear regression together with the solar radio flux as second parameter. The derived regression coefficients are  $C_{solar} = (5.0 \pm 0.7) \text{ K (100 SFU)}^{-1}$  and  $C_{hale} = (1.8 \pm 0.5) \text{ K (100 } \mu\text{T)}^{-1}$  ( $r^2 = 0.71$ ). Secondly, an 24-year independent oscillation is used instead of the Hale cycle, which leads to the best description of the OH\* temperatures series, at all. A multiple linear regression least square fit leads to the coefficients  $C_{solar} = (4.3 \pm 0.7) \text{ K (100 SFU)}^{-1}$  ( $4.1 \pm 0.8) \text{ K (100 SFU)}^{-1}$ ,  $C_{sin} = (1.92 \pm 0.43) \text{ K}$ , and  $C_{cos} = (0.34 \pm 0.42) \text{ K}$  ( $r^2 = 0.77$ ). The amplitude of the 24-year oscillation is  $A = (1.95 \pm 0.43) \text{ K}$  ( $A = \sqrt{C_{sin}^2 + C_{cos}^2}$ ).  $C_{sin} = (1.95 \pm 0.44) \text{ K}$  for the amplitude, and  $P = (24.8 \pm 2.1) \text{ years}$  for the period. The most important point here is that no additional linear trend is needed and that the combination of 24 25-year oscillation and 11-year solar cycle explains all long term dynamics. This is especially satisfying as the notion “trend break” is somewhat “non-physical”.

4. ~~After detrending the temperature series regarding the 11-year solar cycle and the 24-year oscillation MAOs remain. Harmonic fits to the detrended temperature series lead to oscillations with periods of  $P = (2.69 \pm 0.06)$  years,  $P = (3.15 \pm 0.07)$ , and  $P = (4.54 \pm 0.17)$  years with corresponding amplitudes of  $A = (1.03 \pm 0.33)$  K,  $A = (1.03 \pm 0.33)$  K, and  $A = (0.91 \pm 0.36)$  K, respectively.~~
- 5 4. ~~A caveat arises~~ Caution has to be applied when estimating linear trends from data sets containing long term variations. Trend results are quite sensitive to the length of the data interval used. ~~This is especially important for any kind of comparison.~~ In such a case a piecewise linear trend approach has to be used or the long term variation has to be described in another appropriate way, e.g. by using an oscillation.

*Acknowledgements.* This work was funded by the German Federal Ministry of Education and Research (BMBF) within the ROMIC (Role Of the Middle atmosphere In Climate) project MALODY (Middle Atmosphere LOng term Dynamics) under Grant no. 01LG1207A. Wilcox Solar Observatory data used in this study was obtained via the web site <http://wso.stanford.edu> at 2016:04:11\_08:31:21 PDT courtesy of J.T. Hoeksema. The Wilcox Solar Observatory is currently supported by NASA. The solar radio flux 10.7cm data was obtained from the Natural Resources Canada, Space Weather Canada website: <http://www.spaceweather.gc.ca/>.

## References

- Baker, D.J., and Stair Jr., A.T.: Rocket measurements of the altitude distributions of the hydroxyl airglow, *Phys. Scr.*, 37, 611, doi:10.1088/0031-8949/37/4/021, 1998.
- Beig, G.: Long term trends in the temperature of the mesosphere/lower thermosphere region: 2. Solar response, *J. Geophys. Res.*, 116, A00H12, doi:10.1029/2011JA016766, 2011a.
- Beig, G.: Long term trends in the temperature of the mesosphere/lower thermosphere region: 1. Anthropogenic influences, *J. Geophys. Res.*, 116, A00H11, doi:10.1029/2011JA016646, 2011b.
- Bittner, M., Offermann, D., and Graef, H.H.: Mesopause temperature variability above a midlatitude station in Europe, *J. Geophys. Res.*, 105, 2045–2058, doi:10.1029/1999JD900307, 2000.
- 10 Bittner, M., Offermann, D., Graef, H.H., Donner, M., and Hamilton, K.: An 18-year time series of OH\* rotational temperatures and middle atmosphere decadal variations, *J. Atmos. Sol. Terr. Phys.*, 64, 1147–1166, doi:10.1016/S1364-6826(02)00065-2, 2002.
- Coughlin, K., and Tung, K.K.: Eleven-year solar cycle signal throughout the lower atmosphere, *J. Geophys. Res.*, 109, D21105, doi:http://dx.doi.org/10.1029/2004JD004873, 2004a.
- Coughlin, K.T., and Tung, K.K.: 11-Year solar cycle in the stratosphere extracted by the empirical mode decomposition method, *Adv. Space Res.*, 34, 323–329, doi:http://dx.doi.org/10.1016/j.asr.2003.02.045, 2004b.
- 15 Cumming, A., Marcy, G.W., and Butler, R.P.: The lick planet search: detectability and mass thresholds, *Astrophysical Journal*, 526, 890–915, doi:10.1086/308020, 1999.
- Hall, C.M., Dyrland, M.E., Tsutsumi, M., and Mulligan, F.J.: Temperature trends at 90 km over Svalbard, Norway (78° N 16° E), seen in one decade of meteor radar observations, *J. Geophys. Res.*, 117, D08104, doi:10.1029/2011JD017028, 2012.
- 20 Horne, J.H., and Baliunas, S.L.: A prescription for period analysis of unevenly sampled time series, *Astrophysical Journal*, 302, 757–763, 1986.
- Höppner, K., and Bittner, M.: Evidence for solar signals in the mesopause temperature variability?, *J. Atmos. Sol. Terr. Phys.*, 69, 431–448, doi:10.1016/j.jastp.2006.10.007, 2007.
- Jarvis, M.J.: Planetary wave trends in the lower thermosphere – Evidence for 22-year solar modulation of the quasi 5-day wave, *J. Atmos. Sol. Terr. Phys.*, 68, 1902–1912, doi:10.1016/j.jastp.2006.02.014, 2006.
- 25 King, J.W., Hurst, E., Slater, A.J., Smith, P.A., and Tamkin, B.: Agriculture and sunspots, *Nature*, 252, 1974.
- King, J.W.: Sun-weather relationships, *Aeronautics and Astronautics*, 13, 10–19, 1975.
- Lastovicka, J., Solomon, S.C., and Qian, L.: Trends in the Neutral and Ionized Upper Atmosphere, *Space Sci. Rev.*, 168, 113–145, doi:10.1007/s11214-011-9799-3, 2012.
- 30 Lomb, N.R.: Least-squares frequency analysis of unequally spaced data, *Astrophysics and Space Science*, 39, 447–462, 1976.
- Miyahara, H., Yokoyama, Y., and Masuda, K.: Possible link between multi-decadal climate cycles and periodic reversals of solar magnetic field, *Earth and Planetary Science Letters*, 272, 290–295, doi:10.1016/j.epsl.2008.04.050, 2008.
- Mursula, K., and Zieger, B.: Long term north-south asymmetry in solar wind speed inferred from geomagnetic activity: A new type of century-scale solar oscillation, *Geophys. Res. Lett.*, 28, 95–98, doi:10.1029/2000GL011880, 2001.
- 35 Oberheide, J., Offermann, D., Russell III, J.M., and Mlynczak, M.G.: Intercomparison of kinetic temperature from 15  $\mu\text{m}$  CO<sub>2</sub> limb emissions and OH\*(3,1) rotational temperature in nearly coincident air masses: SABER, GRIPS, *Geophys. Res. Lett.*, 33, L14811, doi:10.1029/2006GL026439, 2006.

- Offermann, D., Donner, M., Knieling, P. and Naujokat, B.: Middle atmosphere temperature changes and the duration of summer, *J. Atmos. Sol. Terr. Phys.*, 66, 437–450, doi:10.1016/j.jastp.2004.01.028, 2004.
- Offermann, D., Jarisch, M., Donner, M., Steinbrecht, W., and Semenov, A.I.: OH temperature re-analysis forced by recent variance increases, *J. Atmos. Sol. Terr. Phys.*, 68, 1924–1933, doi:10.1016/j.jastp.2006.03.007, 2006.
- 5 Offermann, D., Gusev, O., Donner, M., Forbes, J.M., Hagan, M., Mlynczak, M.G., Oberheide, J., Preusse, P., Schmidt, H., and Russel III, J.M.: Relative intensities of middle atmosphere waves, *J. Geophys. Res.*, 114, D06110, doi:10.1029/2008JD010662, 2009.
- Offermann, D., Hoffmann, P., Knieling, P., Koppmann, R., Oberheide, J., and Steinbrecht, W.: Long-term trend and solar cycle variations of mesospheric temperature and dynamics, *J. Geophys. Res.*, 115, D18127, doi:10.1029/2009JD013363, 2010.
- Offermann, D., Wintel, J., Kalicinsky, C., Knieling, P., Koppmann, R., and Steinbrecht, W.: Long-term development of short-period gravity waves in middle Europe, *J. Geophys. Res.*, 116, D00P07, doi:10.1029/2010JD015544, 2011.
- 10 Offermann, D., Goussev, O., Kalicinsky, C., Koppmann, R., Matthes, K., Schmidt, H., Steinbrecht, W., and Wintel, J.: A case study of multi-annual temperature oscillations in the atmosphere: Middle Europe, *J. Atmos. Sol. Terr. Phys.*, 135, 1–11, doi:10.1016/j.jastp.2015.10.003, 2015.
- Perminov, V.I., Semenov, A.I., Medvedeva, I.V., and Zheleznov, Yu.A.: Variability of mesopause temperature from hydroxyl airglow observations over mid-latitude sites, Zvenigorod and Tory, Russia, *Adv. Sp. Res.*, 54, 2511–2517, doi:10.1016/j.asr.2014.01.027, 2014.
- 15 Qu, W., Zhao, J., Huang, F., and Deng, S.: Correlation between the 22-year solar magnetic cycle and the 22-year quasicycle in the Earth's atmospheric temperature, *Astronomical Journal*, 144:6, doi:http://dx.doi.org/10.1088/0004-6256/144/1/6, 2012.
- Ryan, S.E., and Porth, L.S.: A tutorial on the piecewise regression approach applied to bedload transport data, Gen. Tech. Rep., RMRS-GTR-189, Fort Collins, CO: U.S. Department of Agriculture, Forest Service, Rocky Mountain Research Station, 2007.
- 20 Scafetta, N., and West, B.J.: Estimated solar contribution to the global surface warming using the ACRIM TSI satellite composite, *Geophys. Res. Lett.*, 32, L18713, doi:10.1029/2005GL023849, 2005.
- Scargle, J.D.: Studies in astronomical time series analysis. II. Statistical aspects of spectral analysis of unevenly spaced data, *Astrophysical Journal*, 263, 835–853, 1982.
- Scherrer, P.H., Wilcox, J.M., Svalgaard, L., Duvall, T.L., Jr., Dittmeier, P.H., and Gustafson, E.K.: The mean magnetic field of the sun - Observations at Stanford, *Sol. Phys.*, 54, 353–361, 1977.
- 25 Schmidt, C., Höppner, K., and Bittner, M.: A ground-based spectrometer equipped with an InGaAs array for routine observations of OH(3-1) rotational temperatures in the mesopause region, *J. Atmos. Sol. Terr. Phys.*, 102, 125–139, doi:10.1016/j.jastp.2013.05.001, 2013.
- She, C.-Y., Krueger, D.A., and Yuan, T.: Long-term midlatitude mesopause region temperature trend deduced from quarter century (1990–2014) Na lidar observations, *Ann. Geophys.*, 33, 363–369, doi:10.5194/angeocom-33-363-2015, 2015.
- 30 Svalgaard, L., Cliver, E.W., and Kamide, Y.: Sunspot cycle 24: Smallest cycle in 100 years?, *Geophys. Res. Lett.*, 32, L01104, doi:http://dx.doi.org/10.1029/2004GL021664, 2005.
- Schwarzenberg-Czerny, A.: The distribution of empirical periodograms: Lomb-Scargle and PDM spectra, *Mon. Not. R. Astron. Soc.*, 301, 831–840, doi:10.1111/j.1365-8711.1998.02086.x, 1998.
- Thomas, S.R., Owens, M.J., and Lockwood, M.: The 22-year Hale cycle in cosmic ray flux – Evidence for direct heliospheric modulation, *Solar Phys.*, doi:10.1007/s11207-013-0341-5, 2013.
- 35 Townsend, R.H.D.: Fast calculation of the Lomb-Scargle periodogram using graphics processing units, *Astrophysical Journal Supplement Series*, 191, 247–253, doi:10.1088/0067-0049/191/2/247, 2010.

- Wei, M., Qiao, F., and Deng, J.: A Quantitative Definition of Global Warming Hiatus and 50-Year Prediction of Global-Mean Surface Temperature, *J. Atmos. Sciences*, 72, 3281–3289 doi:<http://dx.doi.org/10.1175/JAS-D-14-0296.1>, 2015.
- White, W.B., Lean, J., Cayan, D.R., and Dettinger, M.D.: Response of global upper ocean temperature to changing solar irradiance, *J. Geophys. Res.*, 102, 3255–3266, doi:10.1029/96JC03549, 1997.
- 5 Willet, H.C.: Recent statistical evidence in support of predictive significance of solar-climatic cycles, *Monthly Weather Review*, 102, 679, 1974.
- Zechmeister, M., and Kürster, M.: The generalised Lomb-Scargle periodogram - A new formalism for the floating-mean and Keplerian periodograms, *Astronomy and Astrophysics*, 496, 577–584, doi:10.1051/0004-6361:200811296 , 2009.
- Zieger, B., and Mursula, K.: Annual variation in near-Earth solar wind speed: Evidence for persistent north-south asymmetry related to solar magnetic polarity, *Geophys. Res. Lett.*, 25, 841–844, doi:10.1029/98GL50414, 1998.
- 10

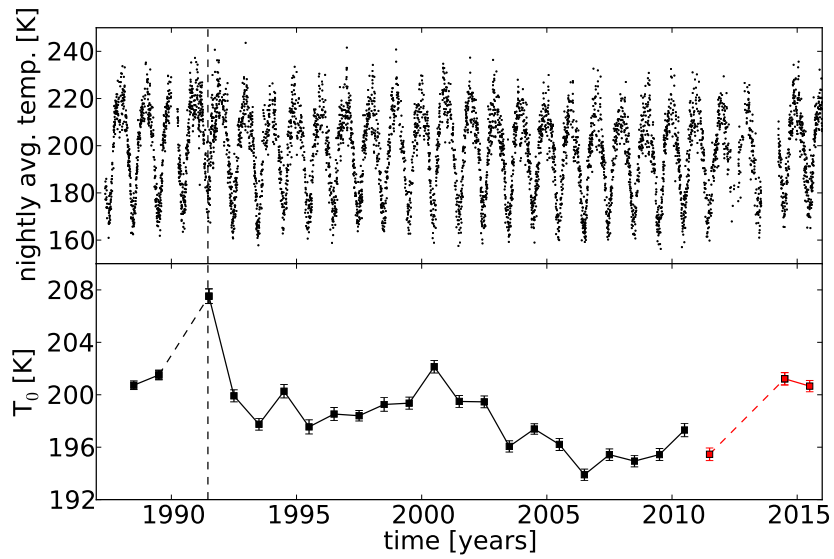


**Figure 1.** OH\* temperature time series derived from GRIPS-II and GRIPS-N measurements at Wuppertal. The upper panel shows the nightly average temperatures and the lower panel shows the annual average temperatures  $T_0$ . Each  $T_0$  is plotted in the middle of the corresponding year and the dates given at the x-axis show the beginning of the years. The annual average temperatures partly or completely derived from the new instrument between 2011 and 2015 are shown in red in the lower panel. The error bars show the estimated standard deviation of the fit parameter. The vertical dashed line marks the date of Mt. Pinatubo eruption.

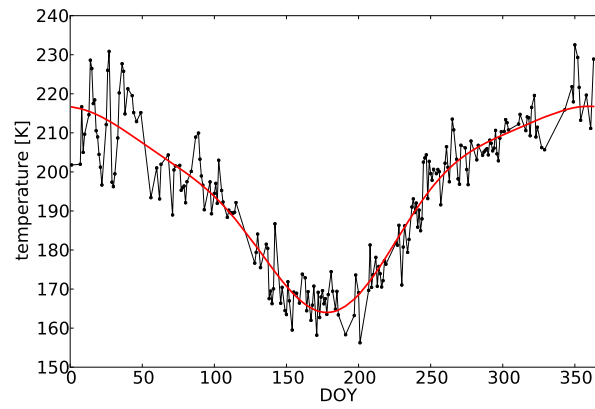


**Figure 2.** GRIPS-II nightly average temperatures of 2009 plotted at the day of year (DOY). The measurement data are shown in black and the harmonic fit using Eq. 1 is shown as the red curve.

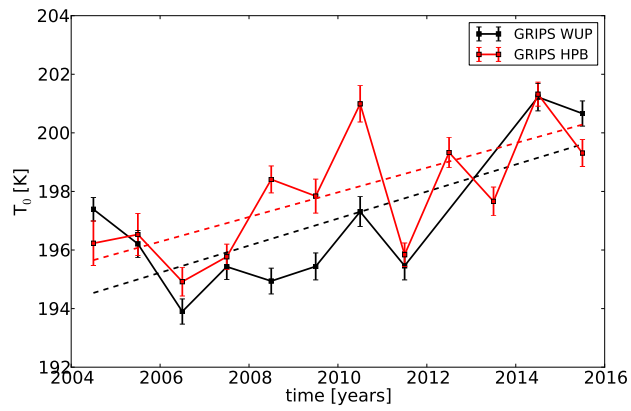


**Figure 3.** OH\* annual average temperatures for the two stations Wuppertal and Hohenpeissenberg in the time interval 2004–2015. The temperatures for Wuppertal (WUP) are shown in black and the temperatures for Hohenpeissenberg (HPB) in red. The dashed lines show the linear fits to the corresponding time series. The linear fit for the Hohenpeissenberg time series only considers measurements at times Wuppertal measurements are also available.

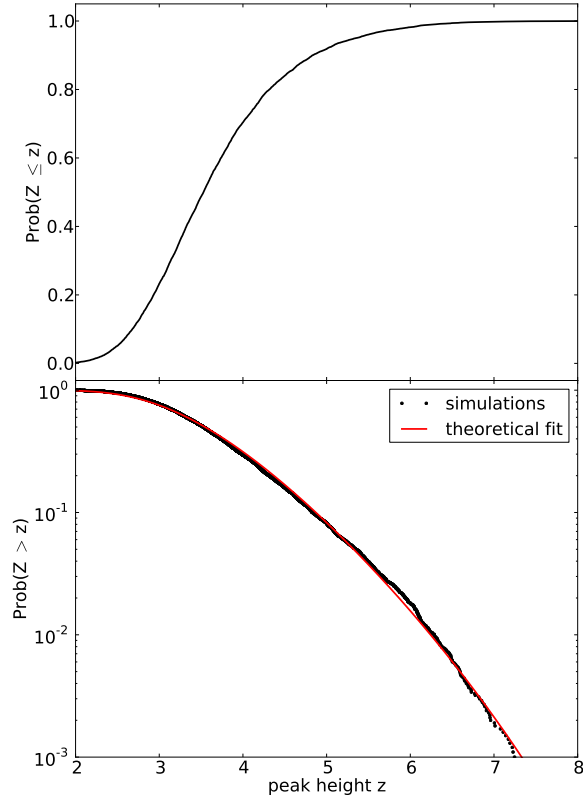


**Figure 4.** Distribution for peak heights  $z$  determined using random values from a gaussian distribution as input for the calculation of LSP (for details see Sect. 3). The upper panel shows the empirical CDF, thus, the probability that there is a height  $Z$  smaller or equal to  $z$ . The FAP (probability that a height  $Z$  larger  $z$  occurs just by chance) is shown in the lower panel. The simulation results are shown in black and a fit to the theoretical curve from Eq. 2 is shown in red. Note the logarithmic scale of the y-axis of the lower panel. This calculations are done for a data sampling same as that of the time series from 1988 to 2015 including data gaps. The fit leads to a number of independent frequencies  $N_i = 32.4$ .

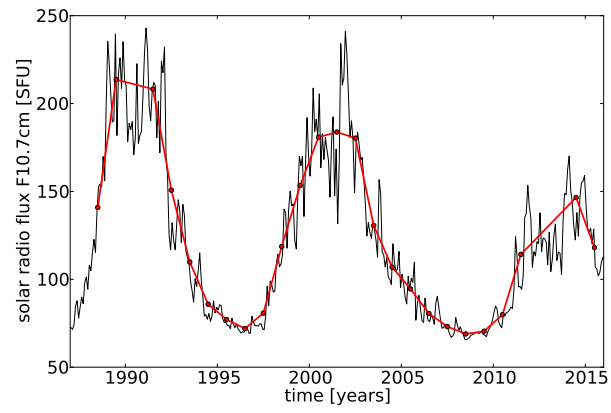


**Figure 5.** Monthly average values of the solar radio flux F10.7cm. The red dots mark the annual average values corresponding to the times of the GRIPS data points. The data were provided by Natural Resources Canada, Space Weather Canada.

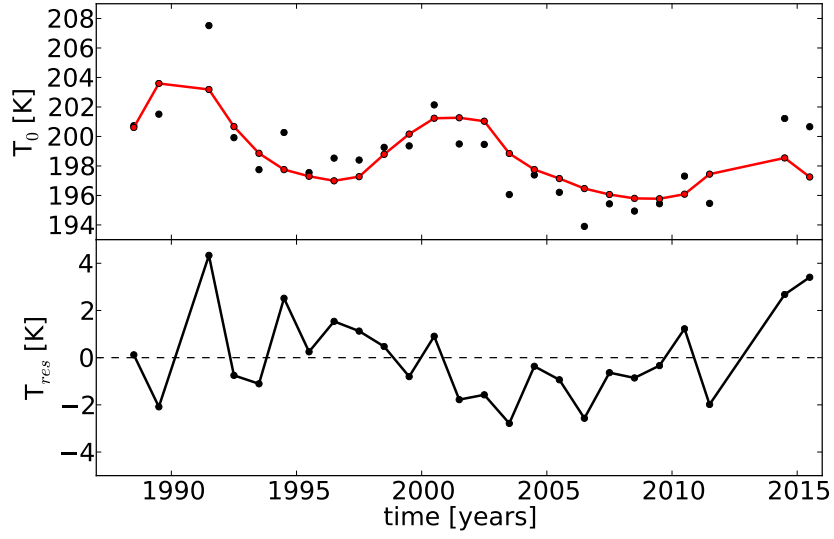


**Figure 6.** The upper panel of the figure shows the time series of annual average OH\* temperatures in black and the fit corresponding to Eq. 3 with the regression coefficients  $C_{trend} = (0.089 \pm 0.055) \text{ K year}^{-1}$  and  $C_{solar} = (4.2 \pm 0.9) \text{ K (100 SFU)}^{-1}$  in red. In the lower panel the residual  $T_{res}$  of the two is shown.

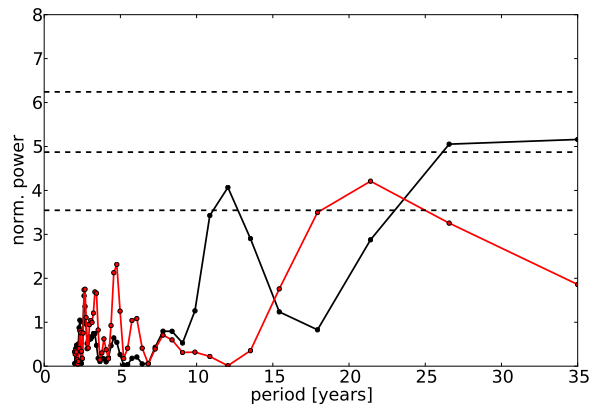


**Figure 7.** The Lomb-Scargle periodogram for the time series of annual OH\* temperatures (see Fig. 1 lower panel) is shown in black and the LPS for the residual after subtracting the fit according to Eq. 3 (see Fig. 6 lower panel) is shown in red. The LSP is evaluated at 53 evenly spaced frequencies in the range  $f = 1/2 \text{ year}^{-1}$  to  $f = 1/35 \text{ year}^{-1}$ . The dashed black horizontal lines display the levels for false alarm probabilities of 0.01, 0.1, and 0.5 (top to bottom), respectively. The false alarm probabilities are calculated according to Eq. 2 using  $N_i = 32.4$  and the number of data points  $N = 25$ .

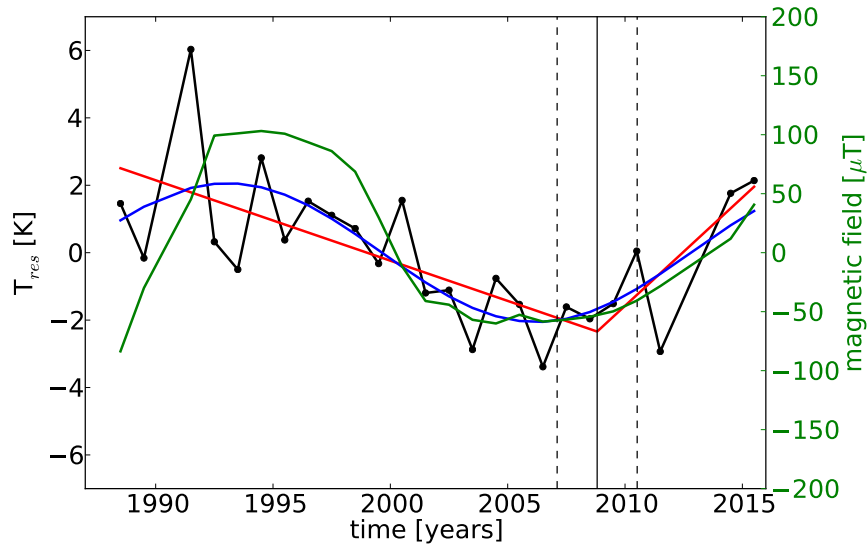


**Figure 8.** Residual for the temperature time series after removing the 11-year solar cycle ( $C_{solar} = (3.3 \pm 0.9) \text{ K } (100 \text{ SFU})^{-1}$ ) and subtracting the mean. The red lines show the fit according to Eq. 7 and the blue curve the fit according to Eq. 8. The break point BP is marked by the vertical black line and the corresponding uncertainties are shown as vertical dashed black lines. Additionally, the solar polar magnetic field is displayed as green curve with a second axis to the right. Shown are the average values for the solar north and south pole with the magnetic field orientation of the north pole. The data were provided by the Wilcox Solar Observatory (for an instrument description see Scherrer et al. , 1977).

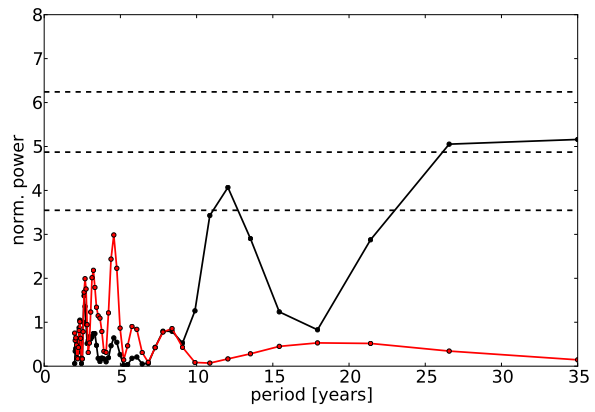


**Figure 9.** The Lomb-Scargle periodogram for the time series of annual OH\* temperatures (see Fig. 1 lower panel) is shown in black and the LPS for the residual after subtracting the fit according to Eq. 4 is shown in red. For details see description of Fig. 7.

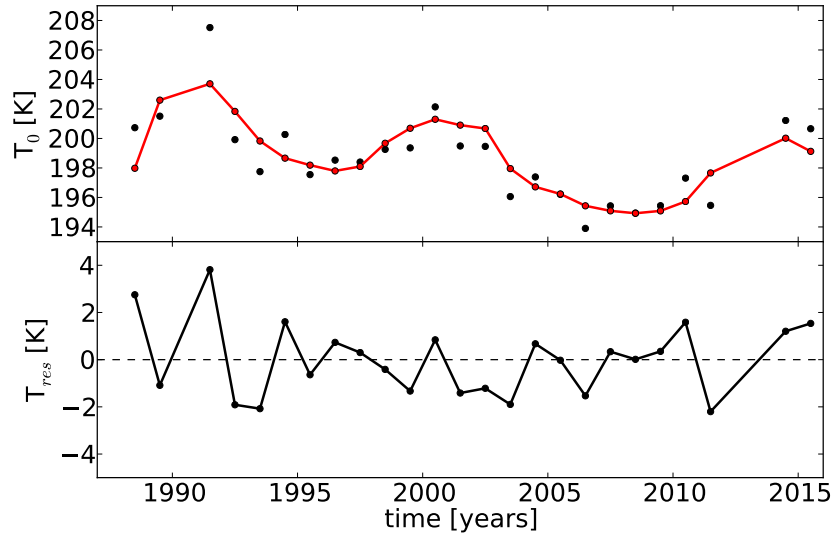


**Figure 10.** The upper panel of the figure shows the time series of annual average OH\* temperatures in black and the fit corresponding to Eq. 9 with the regression coefficients  $C_{\text{halo}} = (1.8 \pm 0.5) \text{ K } (100 \mu\text{T})^{-1}$  and  $C_{\text{solar}} = (5.0 \pm 0.7) \text{ K } (100 \text{ SFU})^{-1}$  in red. In the lower panel the residual  $T_{\text{res}}$  of the two is shown.

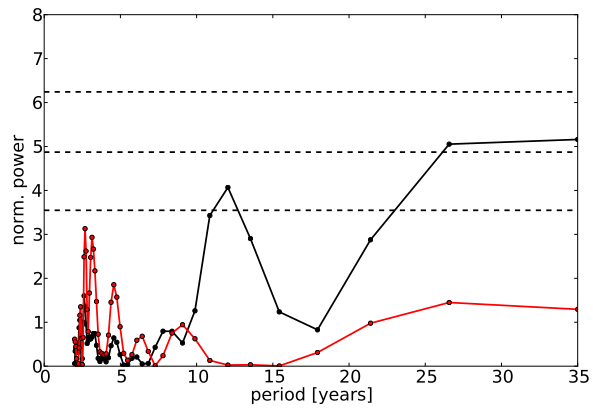


**Figure 11.** The Lomb-Scargle periodogram for the time series of annual OH\* temperatures (see Fig. 1 lower panel) is shown in black and the LPS for the residual after subtracting the fit according to Eq. 9 (see Fig. 10 lower panel) is shown in red. For details see description of Fig. 7.

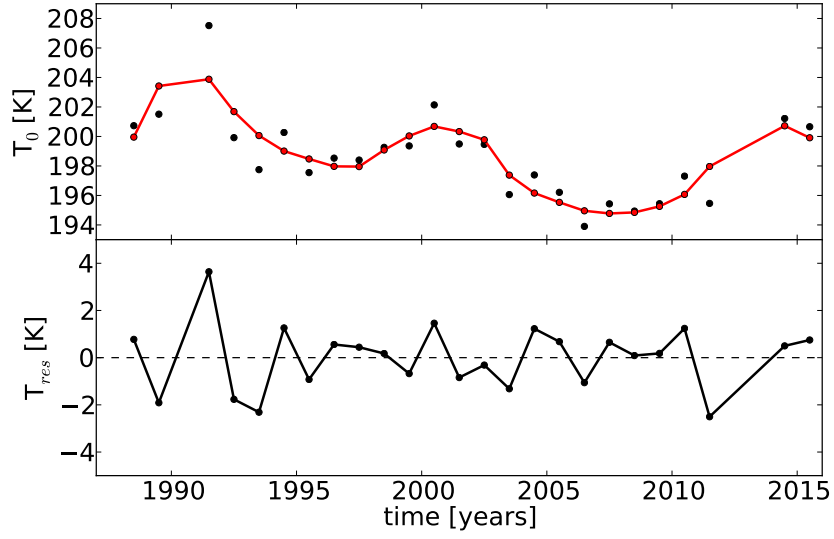


**Figure 12.** The upper panel of the figure shows the time series of annual average OH\* temperatures in black and the fit corresponding to Eq. 10 with the regression coefficients  $C_{solar} = (4.3 \pm 0.7) \text{ K} (100 \text{ SFU})^{-1}$ ,  $C_{sin} = (1.92 \pm 0.43) \text{ K}$  and  $C_{cos} = (0.34 \pm 0.42) \text{ K}$   $(4.1 \pm 0.8) \text{ K} (100 \text{ SFU})^{-1}$ ,  $C_{sin} = (1.95 \pm 0.44) \text{ K}$ , and  $P = (24.8 \pm 2.1) \text{ years}$  in red. In the lower panel the residual  $T_{res}$  of the two is shown.

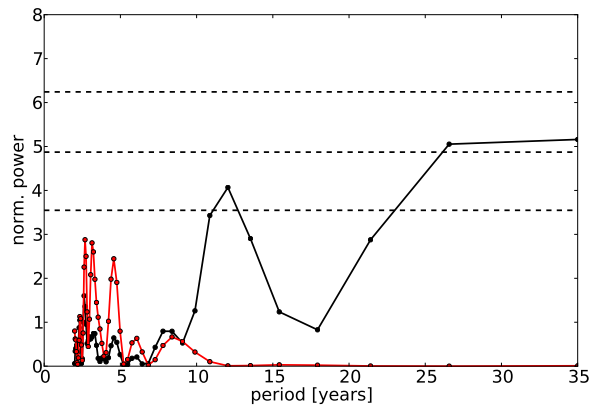


**Figure 13.** The Lomb-Scargle periodogram for the time series of annual OH\* temperatures (see Fig. 1 lower panel) is shown in black and the LPS for the residual after subtracting the fit according to Eq. 10 (see Fig. 12 lower panel) is shown in red. For details see description of Fig. 7.

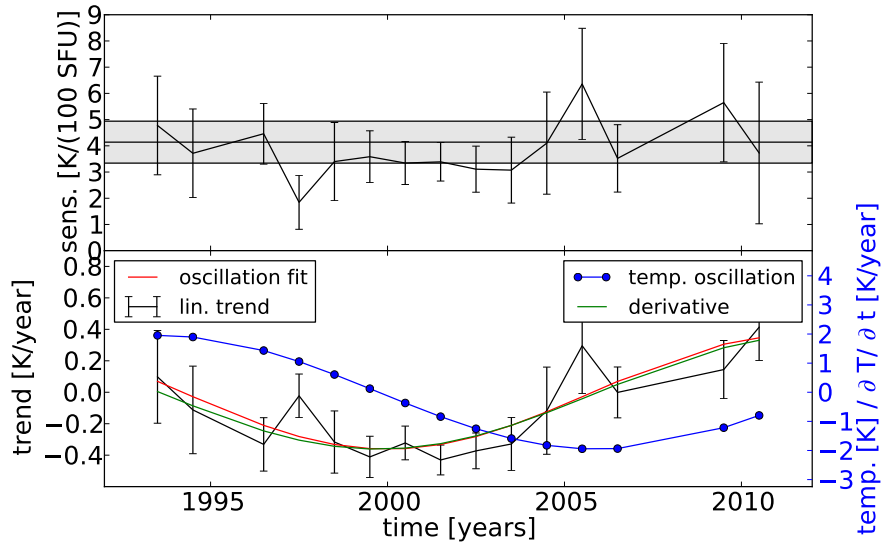


**Figure 14.** The upper panel shows the sensitivity to the solar activity derived for different 11-year time intervals. All values are displayed at the middle of the corresponding time interval. The error bars show the standard error of the fit parameter. The grey shaded area marks the range of the sensitivity derived in Sect. 4.3 for the best fit ( $C_{solar} = (4.1 \pm 0.8) \text{ K } (100 \text{ SFU})^{-1}$ ).

The lower panel of the figure shows the corresponding linear trends for each time interval in black. A sinusoid fitted to these values is shown in red. The result for the 25-year temperature oscillation (see Sect. 4.3) is shown as blue curve and the corresponding derivative of the oscillation is shown as green curve with a second axis to the right.

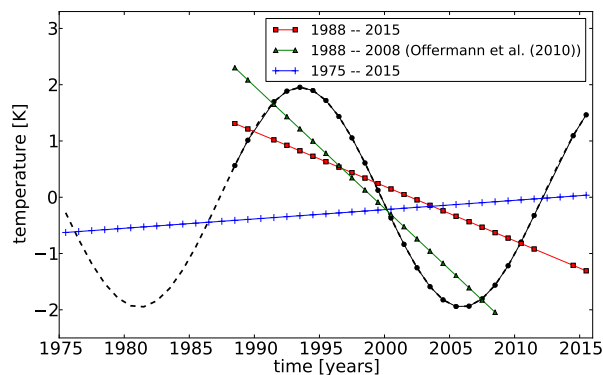


**Figure 15.** 24 25-year oscillation of OH\* temperatures resulting from the multiple-linear-regression least square fit using Eq. 10. The regression coefficients are  $C_{sin} = (-1.92 \pm 0.43)$  K and  $C_{cos} = (0.34 \pm 0.42)$  K. The amplitude of the 24-year oscillation is  $A = (1.95 \pm 0.43)$  K ( $A = \sqrt{C_{sin}^2 + C_{cos}^2}$ ).  $C_{sin} = (1.95 \pm 0.44)$  K, and  $P = (24.8 \pm 2.1)$  years. The solid black line (with full circles) shows the oscillation for the analysed time interval 1988–2015 and the dashed black line shows the continuation of this oscillation back to 1975. The red line (with squares) displays a linear fit to the oscillation for the time interval 1988–2015, the green line (with triangles) the fit for the interval 1988–2008, and the blue line (with plus signs) a fit to the interval 1975–2015.